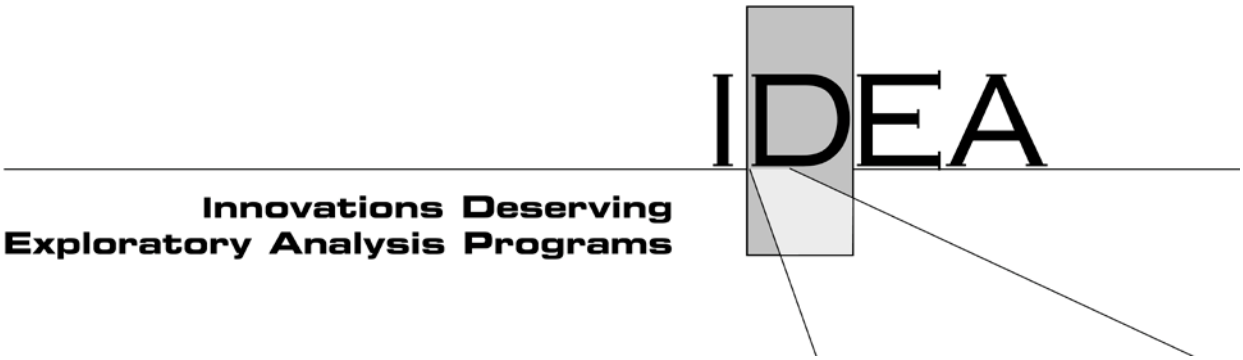

NCHRP IDEA Program

Achieving Resilient Multi-Span Bridge by using Buckling-Restrained Braces

Final Report for
NCHRP IDEA Project 215

Prepared by:
Homero Carrion-Cabrera
Michel Bruneau
University at Buffalo

December 2022

NATIONAL ACADEMIES Sciences Engineering Medicine

TRB TRANSPORTATION RESEARCH BOARD

Innovations Deserving Exploratory Analysis (IDEA) Programs Managed by the Transportation Research Board

This IDEA project was funded by the NCHRP IDEA Program.

The TRB currently manages the following three IDEA programs:

- The NCHRP IDEA Program, which focuses on advances in the design, construction, and maintenance of highway systems, is funded by American Association of State Highway and Transportation Officials (AASHTO) as part of the National Cooperative Highway Research Program (NCHRP).
- The Safety IDEA Program currently focuses on innovative approaches for improving railroad safety or performance. The program is currently funded by the Federal Railroad Administration (FRA). The program was previously jointly funded by the Federal Motor Carrier Safety Administration (FMCSA) and the FRA.
- The Transit IDEA Program, which supports development and testing of innovative concepts and methods for advancing transit practice, is funded by the Federal Transit Administration (FTA) as part of the Transit Cooperative Research Program (TCRP).

Management of the three IDEA programs is coordinated to promote the development and testing of innovative concepts, methods, and technologies.

For information on the IDEA programs, check the IDEA website (www.trb.org/idea). For questions, contact the IDEA programs office by telephone at (202) 334-3310.

IDEA Programs
Transportation Research Board
500 Fifth Street, NW
Washington, DC 20001

Achieving Resilient Multi-Span Bridge by using Buckling-Restrained Braces

NCHRP IDEA Program Final Report

IDEA Project NCHRP-215

Prepared for the IDEA Program
Transportation Research Board
The National Academies of Sciences, Engineering, and Medicine

by

Homero Carrion-Cabrera, Michel Bruneau

University at Buffalo

December 2022

ACKNOWLEDGEMENT

This study was sponsored by the Transportation Research Board of the National Academies under the TRB-IDEA Program (NCHRP-215). The Fulbright program, SENESCYT Ecuador, and the University of Buffalo, are also acknowledged for their financial support through a scholarship to Homero Carrion Cabrera. This research was also made possible thanks to the significant donations of material and in-kind donations from the American Institute of Steel Construction, the High Industries Inc. companies (High Steel, High Concrete, and High Transit), CoreBrace LLC, and RJ Watson Inc. However, any opinions, findings, conclusions, and recommendations presented are those of the authors and do not necessarily reflect the views of the sponsors.

Contents

GLOSSARY

AASHTO	American Association of State Highway and Transportation Officials
AISC	American Institute of Steel Construction
BRB	Buckling Restrained Braces
CQC	Complete Quadratic Combination
DTO	Department of Transportation
ELF	Equivalent Lateral Forces
NL-RHA	Nonlinear Response History Analysis
RSA	Response Spectrum Analysis
SDOF	Simple Degree of Freedom
SEESL	Structural Engineering and Earthquake Simulation Laboratory
UB	University at Buffalo

EXECUTIVE SUMMARY

The objective of this NCHRP-IDEA Type 2 project was to make the bidirectional ductile end diaphragm concept applicable to common multi-span bridges as a way to prevent damage in their substructure and superstructure due to earthquake excitation. The concept uses energy-dissipating buckling restrained braces (BRB) as "fuses" or sacrificial elements located at the end of the superstructure's floating spans. The viability of the concept was initially demonstrated in a NCHRP-IDEA Type 1 project for single-span bridges. Figure E1 shows different configurations of the energy dissipation system. The current project successfully expanded the concept to multi-span bridges through analytical and experimental research. Therefore, findings from this project will allow to expand the use of ductile end diaphragms (already implemented in the AASHTO Guide Specification for LRFD Seismic Bridge Design but limited only to transverse excitation applications), to provide resistance to bidirectional excitation, in multi-span bridge configurations. This innovative system using BRBs can provide seismic resilient and damage-free bridges applicable to different levels of seismic forces at low cost as a result of the availability of BRBs in different capacities ranging from 20 to 1,400 kips and already tested for building use purposes.

Two main problems that prevented the implementation and broad use of this concept were addressed in this project: (1) the need to understand analytically the behavior of the system in a multi-span configuration, to be able to propose a simple design procedure; and (2) the need to validate experimentally BRB connections to demonstrate their ability to work under 3-D displacements imposed due to the inclination of BRBs.

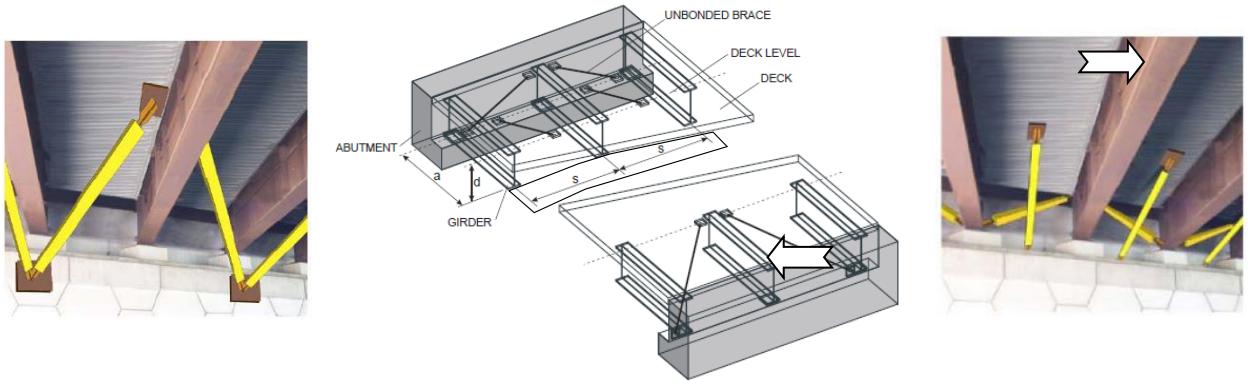

Figure E1: Conceptual illustration of the bidirectional diaphragm with two possible configurations.

This was done by executing the project in two stages. In Stage 1, multi-span bridges having simply supported spans with the proposed ductile end diaphragms were investigated to understand their seismic behavior, considering various layouts and implementation strategies. Moreover, a parametric analysis considered the influence of different elements of the structure, such as the geometry of piers (represented

by their stiffness), the span mass, and other factors. Two kinds of analyses were conducted in order to determine the level of complexity required to define the design rules. They are modal analysis or response spectrum analysis (RSA), and nonlinear response history analysis (NL-RHA). This was done for two different layouts of BRBs: one layout with BRBs connecting the end of the span to the adjacent bent cap or abutment, as shown in Figure E2), and a second layout with BRBs connecting adjacent spans to each other. After understanding which is the ideal configuration and under what circumstances, BRBs were designed for the selected layout using NL-RHA to reach the optimal performance of uniform ductility in BRBs along the bridge.

Based on results from this optimal design, a design procedure simple enough to achieve adequate seismic performance was proposed. The design procedure results were assessed by subjecting example bridges (regular and irregular) to a suite of ground motions, using NL-RHA. The analysis allowed the research team to investigate the impact of the simple design method on global behavior, as well as to understand the magnitude of the local demands and the magnitude of hysteretic displacements that the BRBs will have to accommodate. A significant part of the project was invested in Stage 1 research because it is of extreme importance to understand adequately how different configurations of BRBs along the bridge can help to dissipate the seismic energy proportionally across all BRBs and in such way that the substructure and the superstructure remain elastic. Finally, the proposed design procedure and results from NL-RHA were used to design the 1/2.5 scale specimen to be tested in the second stage.

During the second stage (Stage 2), a specimen designed in Stage 1 was subjected to shake table testing. Shake table testing is equivalent to field testing, with the advantage that specimens can be excited by ground motions immediately instead of waiting for severe ground motions to validate the design in the field. The specimen, shown in Figure E2, was one part of a 5-span bridge and it represented one span with BRBs connected to the abutment and the pier next to it. The main purpose of these tests was to experimentally validate proposed connection details when subjected to the 3-D displacement histories (compared with the axis of the BRBs) that resulted from bidirectional ground motions and the fact that the connections must accommodate inclined BRB layouts. Connections represented the details applicable for a new construction as well as for retrofitting. Tests included earthquake displacement histories that represent design demands (obtained from Stage 1) and combinations of earthquake and thermal excitations; and to make BRB fail, additionally extreme motions that represents pulses, records from soft soils sites, and near field records were used. The test protocols were repeated on each specimen until failure, to establish their ultimate hysteretic capacity. This experimental validation provided the final piece needed to implement the proposed design procedure.

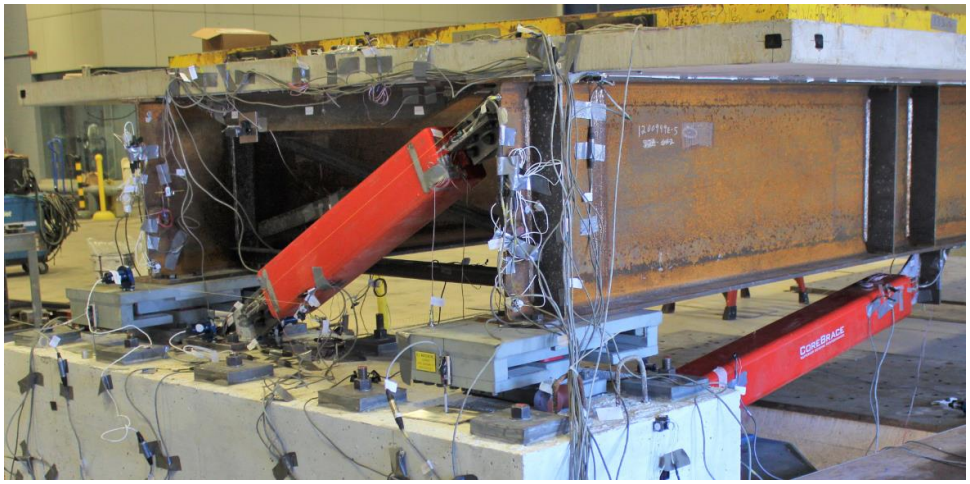

Figure E2: One end of the tested specimen with one of the configurations of BRBs considered

The sum of this research work demonstrated the ability to achieve resilience in ordinary multi-span bridges by using inexpensive BRBs. In contrast with the large seismic displacements that must be accommodated by special expansion joints when using base isolation solutions, the proposed concept results in small displacements that can be accommodated by regular expansion joints. Another advantage of the concept is its simplicity, which makes it an attractive solution for seismic design for all seismic regions and applicable to routine designs, avoiding expensive peer reviews. The way that BRBs are to be located along a bridge also makes them easy to repair (although unlikely needed), avoiding closure of the bridge in case of needed substitution after an earthquake. Finally, considering the simplicity of the concept, it also makes for an economical and rapid scheme for bridge retrofit.

IDEA PRODUCT

Bidirectional ductile Diaphragms provide an inexpensive solution to achieve resilient damage-free multi-span bridges, for both transverse and longitudinal seismic response. The elimination of bridge closures and repairs following earthquakes can prevent massive economic losses (for example, Enke et al. (2008 estimated partial indirect losses of $703 million, in addition to direct losses, due to bridge damage alone for an earthquake scenario in St. Louis). The simplicity of the proposed concept makes it an attractive solution for seismic design in all seismic regions (the AASHTO seismic maps recognize that the potential for damaging earthquakes exists in over 40 States across the USA). Ductile end diaphragms can be designed to accommodate any level of seismic forces, given that BRBs having capacities ranging from 20 to 1400 kips have already been designed and tested (for the building market). Beyond being a concept for new bridges, in some cases, the solution can also be used to retrofit existing bridges.

This research has produced an “equivalent lateral force” design procedure that can be implemented in AASHTO and Departments of Transportation in their seismic design specifications, to be used by design engineers and consultants.

CONCEPT AND INNOVATION

The term "bidirectional end ductile diaphragms" is used to emphasize that energy dissipation is achieved at the ends of the spans of the superstructure – in this case, using Buckling Restrained Braces (BRBs). This innovative approach can be implemented in both concrete bridges and steel bridges. BRBs with stable and high energy dissipation capacity for seismic applications have been implemented in buildings for over 15 years. Although the bridge industry is lagging, with BRBs only used for the seismic retrofit of long-span bridges in the USA to date (e.g., Foresthill Bridge and Vincent Thomas Bridge), their potential is recognized. There will be substantial benefit to expand the use of BRBs, from limited specific bridge applications to everyday implementation for ordinary standard multi-span bridges.

The design objective of the innovative concept presented here is to achieve resilient bridges, by preventing earthquake damage to both the bridge superstructure and substructure. This aligns with important strategic priorities of many Departments of Transportation (DoTs) that include in their strategic plans a focus on implementing innovative solutions to ensure, sustainability, reliability, and structural integrity. It also eliminates the need for repairs following an earthquake, thus minimizing bridge closures and traffic delays. Current state of practice in seismic design of ordinary multi-span bridges relies either on plastic hinging of columns to dissipate earthquake energy, or on base isolation. The first one implies damage to the gravity-carrying columns; the second one requires special bearings and expansion joints to accommodate displacements that can be extremely large in many cases, as well as a special design procedure (and sometimes peer-review of the design by other engineers). Using the bidirectional ductile diaphragm concept with inexpensive BRBs can provide resilient bridges with damage-free columns, at low cost, while minimizing displacements demands to levels that can be easily accommodated.

BRBs are inexpensive (each costing between $2000 to $5000 for the most commonly used BRB sizes), and durable structural elements built of steel and concrete – materials well understood by practicing engineers. As such, bridges having BRBs can be designed by bridge engineers using conventional structural engineering approaches. Other significant savings result from the fact that the proposed design is intended to eliminate the need for post-earthquake repairs (that often cost a premium in a post-earthquake environment and that typically limit the use of a bridge following an earthquake).

The equivalent lateral force procedure developed as part of this research project provides and expedient way for engineers to design bidirectional ductile diaphragms in multi-span simply supported bridges.

1 INVESTIGATION

1.1 INTRODUCTION

Current state of practice in seismic design of ordinary multi-span bridges generally relies either on plastic hinging of columns to dissipate earthquake energy, or on base isolation. The first one implies damage to the gravity-carrying columns; the second one requires a special bearings and expansion joints to accommodate displacements that can be extremely large in many cases, as well as a special design procedure (and sometimes peer-review of the design by other engineers). Using the bidirectional ductile end diaphragm concept with inexpensive Buckling Restrained Braces (BRBs) can provide resilient bridges with damage-free columns, at low cost, while minimizing displacements demands to levels that can be easily accommodated. The elimination of bridge closures and repairs following earthquakes can prevent massive economic losses (for example, Enke et al. (2008) estimated partial indirect losses of $703 million, in addition to direct losses, due to bridge damage alone for an earthquake scenario in St. Louis). The simplicity of the bidirectional ductile end diaphragm concept makes it an attractive solution for seismic design in all seismic regions (the AASHTO seismic maps recognize that the potential for damaging earthquakes exists in over 40 States across the USA). Ductile end diaphragms can be designed to accommodate any level of seismic forces, given that BRBs having capacities ranging from 20 to 400 kips have already been designed and tested (for the building market). Beyond being a concept for new bridges, in some cases, the solution can also be used to retrofit existing bridges. Therefore, to implement the bidirectional ductile end diaphragm concept with BRBs in codes, this research project studies the concept analytically and experimentally.

Buckling restrained braces (BRB) are special braces capable to yield in axial tension and compression. They allow to achieve large plastic displacements, produce stable hysteretic behavior, and dissipate large amounts of seismic energy – capabilities that are valuable in seismic resisting structures. Initially, these elements were first introduced in buildings in Japan in 1987, in the USA in 1999 (Aiken et al. 1999), and in many other countries since. They are nowadays widely used and design requirements for buckling restrained braced frames are specified by the AISC Seismic Provisions for Structural Steel Buildings (AISC 341 2022). Given that all the yielding in a BRB happens inside its casing, to help structural engineers determine if BRBs should be replaced following an earthquake, some manufacturers have also integrated into their BRBs displacement transducers capable of recording the history of cyclic deformations of the brace yielding core over time; this information can then be used to calculate the BRB remaining fatigue life and avoid premature replacement after major earthquakes and/or several years of service. In bridges, there have been much fewer applications to date. Examples include the Vincent Thomas Bridge (Ingham, Rodriguez, and Nader 1997, Lanning, Benzoni, and Uang 2016a, b, CoreBrace 2021) and the Minato bridge

(Kanaji et al. 2005) which were retrofitted with BRBs. While these were large bridges that were analyzed using Nonlinear Response History Analysis (NL-RHA), there would be benefits in using BRBs to enhance the seismic performance of common bridges, particularly if they could be designed using elastic procedures.

In bridges, before the use of BRBs, several concepts were developed to implement hysteretic energy dissipation devices. One such concept that is considered here is the use of ductile end diaphragms, which consists of hysteretic devices (or "structural fuses") implemented in the diaphragms located at the ends of spans. These ductile end diaphragms are intended to dissipate seismic energy and prevent damage in the substructure by limiting the magnitude of transmitted forces. The concept was initially developed and tested with various hysteretic devices for seismic forces in the transverse direction by Zahrai and Bruneau (1999a, 1999b) and a design procedure provided by Alfawakhiri and Bruneau (2001) has been implemented in AASHTO (2011). Further shake table studies by Carden, Itani, and Buckle (2006) verified the concept by exciting, in their transverse direction, scaled bridges having BRBs as fuse elements at their end diaphragms. Later, the concept was expanded to bidirectional seismic forces for bridges with stiff structures (Celik and Bruneau 2009, Wei and Bruneau 2018) and a design procedure was also provided for the case of rigid piers. The concept of "bidirectional ductile end diaphragm" emphasizes the ability to dissipate energy under both longitudinal and transverse seismic excitations by devices installed at the ends of the span. The advantage of this system is the restriction of displacements between spans, which can be accommodated with low cost expansion joints, and the prevention of damage to substructural elements when bridges are seismically excited in both horizontal directions. Pantelides et al. (2016) studied the application of BRBs in the longitudinal direction to reduce pounding in curved and skewed bridges as a retrofit strategy but did not propose a generally applicable elastic analysis based design procedure.

Currently, if wishing to use BRBs to implement a bidirectional diaphragm strategy, the AASHTO Guide Specification for LRFD Seismic Bridge Design provides simple equations that could be used for the transverse direction, but there is no verified procedure available other than performing NL-RHA to design BRBs in the longitudinal direction. To make the bidirectional diaphragm concept attractive to be applied to multi-span bridges, a design procedure based on elastic analysis is required. Therefore, an analytical understanding was developed here of the behavior of multi-span bridges having simply-supported spans and BRBs tying the spans to each other or to the column bents, and the findings are formulated into a simple design procedure applicable to general multi-span bridges. Then, an experimental program was conducted to validate the concept, using various BRB configurations and BRB end connections to demonstrate their ability to provide their expected ductile behavior while subjected to the full 3-D end displacements that are unique to this type of implementation. This report presents the findings resulting from this research project.

2 ANALYTICAL RESEARCH

2.1 OVERVIEW OF ANALYTICAL RESEARCH CONDUCTED

In this first stage of the research program, ductile end diaphragms equipped with buckling restrained braces (BRB) were designed for non-skew multi-span simply supported bridges using elastic linear analysis and nonlinear response history analysis (NL-RHA) to achieve uniform ductility demand in all BRB along the bridge. All bridges considered floating spans (i.e., on slider bearings providing no effective lateral resistance). Additionally, the number of spans considered ranged from 2 to 11. Two BRB layouts were analyzed elastically for BRBs in the bridge longitudinal direction, and the layout with BRBs connecting the spans to the substructure was found to result in better designs. Consequently, this layout was selected for further design and analysis with NL-RHA. Evaluation with NL-RHA of elastic designs based on response spectrum analysis (RSA) and using simplified material models showed that uniform ductility demand was not achieved; instead, ductility demand concentrated in the BRBs connecting to the abutment and those at mid-length of the bridge. The same conclusion was obtained using different strain hardening material models for the BRBs. Then, bridges were designed with NL-RHA and an optimization procedure to obtain BRBs that reached the same ductility demand along the bridge, showing that such a seismic performance is possible. Based on the BRB cross-section areas obtained from designs with NL-RHA, a simplified design procedure was developed for BRBs in the longitudinal direction, similar to the Equivalent Lateral Force (ELF) procedure used in building. For BRBs in the transverse direction, displacement-based design was found to be an adequate design procedure. With the simplified design procedures, a 5-span regular span bridge was designed with BRBs as a prototype from which the span connecting to the abutment and a bent was selected to design a representative specimen for the shake table experiments to be conducted.

2.2 LONGITUDINAL DIRECTION ANALYSIS AND DESIGN

2.2.1 Elastic design and analysis

Initially, regular bridges were designed in the longitudinal direction based on RSA. The use of the RSA design procedure (also called “multimodal analysis” in AASHTO) is recommended by the AASHTO Guide Specifications for LFRD Seismic Bridge Design (2011) for irregular bridges or regular bridges with more than 6 spans. RSA was deemed adequate to use in all bridges here considering that the bridges analyzed had numbers of spans ranging from 2 to 11, the concept of the bidirectional ductile end diaphragm has not been used before, and results from bridges with a different number of spans were compared between each other. To combine modes, the complete quadratic combination method (CQC) was selected given that periods from different modes are closely spaced between each other. The design spectrum used was for Memphis, Tennessee, and is shown in Figure 2-1. This location was used in the study by Wei and Bruneau (2016), and was selected here to maintain continuity with this previous research. Recall, Memphis was

selected because of its large annual variation in temperature (for demands in BRBs across expansion joints) while being located in a high seismic zone.

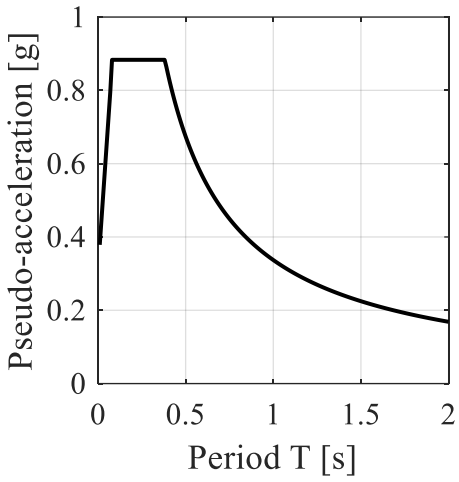

Figure 2-1 Response spectrum

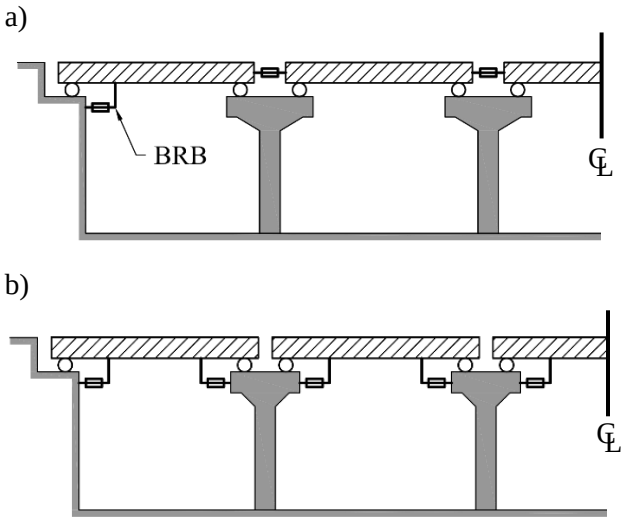

Figure 2-2 Configurations: a) BRBs connecting adjacent spans each other, and; b) BRBs connecting spans to piers and abutment

For the design, it was initially decided to use a response modification factor (R) equal to 5 and BRBs all having the same length of 80". Furthermore, two layouts were analyzed: one with BRBs connecting spans to abutments and to each other avoiding interaction with piers, as shown in Figure 2-2(a); and another with BRBs connecting spans to piers and abutments, as shown in Figure 2-2 (b). (Incidentally, note that everywhere in this report where a BRB area is calculated, this area could be taken as the sum of the areas provided by multiple BRBs if such redundancy is desired, for example by installing a longitudinal BRB under each girder in the longitudinal direction, or by introducing BRBs between all girders in the transverse direction). The model was simplified by considering spans as rigid, lumping their mass at the center of the spans, and assuming zero-friction sliding bearings. Initial design trials showed that the design procedure for each bridge required several iterations to converge to effective BRB areas, especially when piers were flexible. To automate the design procedure, an optimization algorithm was used to design the BRBs.

Results obtained for the case of BRBs connecting spans to each other showed that the BRBs connected to abutments required the largest strength along the bridge, and that when the number of spans was even, the BRBs located at the mid-length of the bridge always experienced zero elongation.

In the case of BRBs connecting spans to piers and abutments, it was observed that the value considered for the piers' stiffness can change the behavior of the bridge. For instance, when piers are rigid each span behaves as a simple degree of freedom (SDOF) system, and when pier are flexible the bridge behaves as a multi-degree of freedom system similar to a chain with multiple links. Thus, several stiffnesses were selected for analyses considering spans of equal weight. The range of stiffnesses considered included the two extreme scenarios of when piers are too flexible and when piers are rigid. Results showed that when piers are semi-rigid or rigid, some of the BRB cross-section areas required were close to zero (or zero). This revealed a flaw in the optimization design procedure. To resolve this issue, and at the same time decrease the number of BRBs having different sections across the bridge, two possible solutions were analyzed: one where the BRBs connected to the same span have the same cross-section area, and another where BRBs connected to the same pier have the same area. Comparing both solutions from a capacity-design point of view, the configuration with BRBs connected to the same pier having the same cross-section area is the one which produces lower demands in the substructure. Therefore, this was used in all subsequent designs. Note that when BRBs connected to the same pier exhibited different ductility demands, only results for the BRB developing the greatest ductility demand was considered in all subsequent comparisons (and is the one used when seeking to reach a target BRB ductility uniformly across the entire bridge).

Finally, the influence of the mass of the span was analyzed by considering different values for the mass of the span. From these analyses, it was observed that the ratio between BRB cross-section area and span mass is constant for a given number of spans and a given ratio of span mass, M_{span}, to pier stiffness, K_{pier}. The ratio of span mass to piers stiffness is represented by the period of the pier (T_p) (note that since the tributary mass of the pier lumped at its top is a percentage of the mass span, it was not considered), which is equal to a constant times the square root of the mentioned ratio and it is represented by Eq. (1).

$$T_p = 2\pi \sqrt{\frac{M_{span}}{K_{pier}}} \tag{1}$$

2.2.2 Nonlinear time history analysis and design

The designs obtained based on elastic analysis were analyzed with NL-RHA to verify if uniform ductility was effectively achieved along the bridge. However, before performing NL-RHA, several parameters were defined. The set of 22 pairs of far-field ground motions from FEMA P695 (2009) and its scaling procedure was used. Considering that the present study is not site-specific, the FEMA P695 set of ground motions was deemed to be the most appropriate and selected here. The inelastic hysteretic response of BRBs was represented using a Menegotto-Pinto model with post-yield stiffness equal to 3% of the initial one, a small

radius in the initial transition from the elastic to the inelastic range, and without isotropic hardening; which depending on the value of the parameter selected, can turn into a bilinear model. The advantage of this model is the smooth transition between the elastic to the inelastic range, avoiding numerical issues (i.e. spurious damping forces) and accounting for the Bauschinger effect in the hysteretic behavior. Piers were modeled as elastic elements because they were not expected to develop yielding, as a consequence of the capacity design approach adopted here. Raleigh damping was used with 5% damping in the first and third mode; although a lower damping could arguably have been used, the value of 5% can be considered to account for additional energy dissipation that would develop in the sliding bearings at the end of each span, which is not explicitly modeled (as idealized friction-less bearings are used in the computer models).

To reduce analysis time, the set of bridges was reduced arbitrarily to bridges with an odd number of spans varying from 3 to 11, equal span mass, and pier stiffness varying from rigid to flexible (equal to T_p ranging from 0.1 to 2 seconds, respectively). Additionally, bridges were designed with RSA for reduction factors, R[1], varying from 2 to 10. Results obtained from bridges with a different number of spans showed that the geometric mean (which represent the median of a lognormal distribution and also called "geomean" here) BRB ductility demand is larger when piers are rigid (as each span behaves as a SDOF in the short period range), and reduced when piers become more flexible, as shown in Figure 2-3a. To unify results, the geomean of all BRB response was obtained, independently of the number of spans and designed with the same R value, resulting in the curves shown in Figure 2-3b, which can be used to approximate the global ductility demand in BRBs. For instances, to get a global median ductility demand equal to 5, the factor R can be defined as

$$R = \begin{cases} 3 & T_p \leq 0.4 \\ 2.33 + 1.67T_p & 0.4 < T_p < 1 \\ 4 & T_p \geq 1 \end{cases} \quad (2)$$

and for ductility of 10, the R value should be between 5 to 6.

[1] The displacement-based design philosophy in the AASHTO Guide Specifications for LRFD Seismic Design is not applied to steel structures/substructures that are intended to be the energy dissipating elements (Section 7 of the Specifications). Throughout Section 7, R factors are used for design. This is because there are a number of challenges in applying the displacement-based design method to steel structures, and these have not been all resolved yet. This has been summarized in NCHRP 949 report "Proposed AASHTO Guidelines for Performance-Based Seismic Bridge Design". It is possible that displacement-based design approaches can be developed for ductile diaphragms at some point in the future, but until then, the R-factor approach is used, and the work performed as part of this research project follows the same approach.

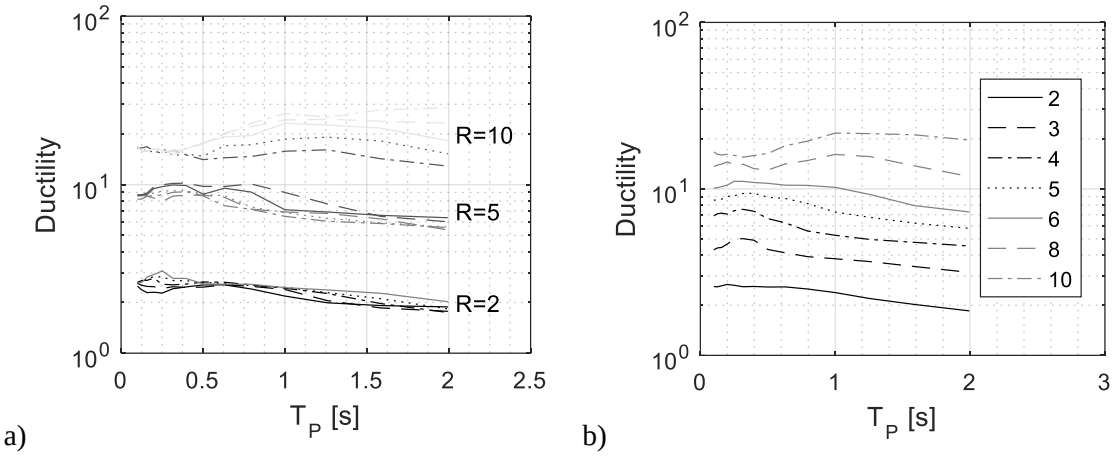

Figure 2-3 Ductility demands as a function of pier stiffness: a) Geometric mean of the geomean of ductility demands for different number of spans and R values; b) average of geomeans of ductility demands for different R values

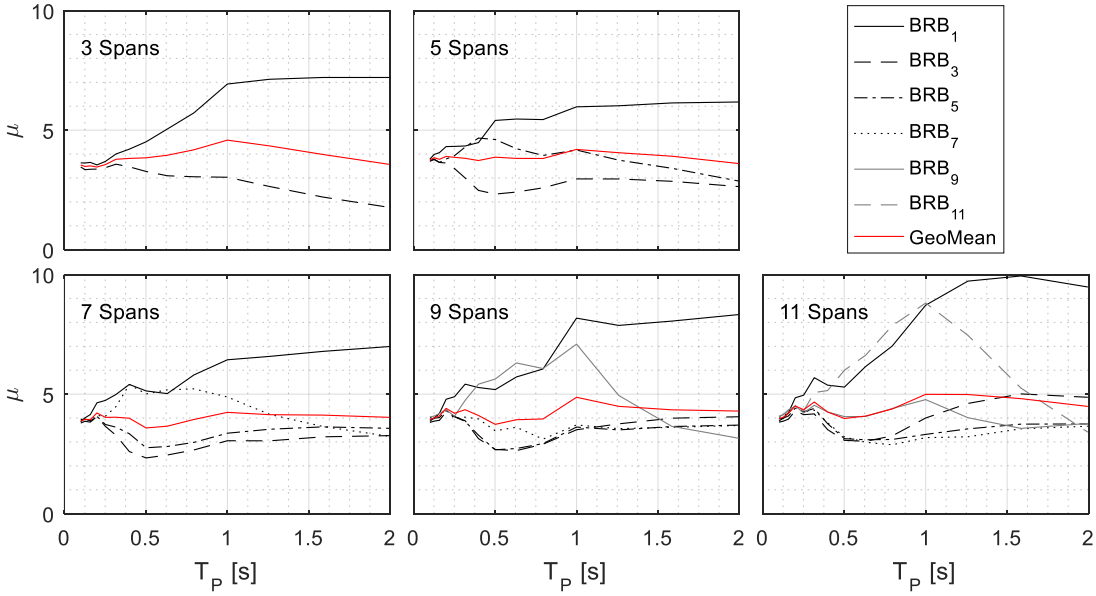

Figure 2-4 Median demand ductility of BRBs for different number of spans and pier stiffnesses

Results for mean ductility demands of bridges designed with RSA and Eq. (2) showed that, except when piers are dominantly rigid, there is a concentration of ductilities in the first BRB. Besides, for models with 5 or more spans, ductility demand also concentrated in BRBs located at the mid-length of the bridge, as shown in Figure 2-4. For some values of pier stiffness, BRBs demand increased by a ductility of 5, but decreased by 2 below the target value for the remaining BRBs.

Several solutions to the problem of concentration of ductility demand were analyzed aiming to distribute ductility demand uniformly along BRBs in the bridge. One option was increasing artificially the strength and stiffness of the BRB by 25% at the location where large ductilities were obtained. This effectively reduced the concentration of ductility demand but increased demand in other members. Another solution was to improve the material model to account for strain hardening. The Bouc-Wen model and the Menegotto Pinto model modified by Filippou (material defined as SteelMPF in OpenSees (2000)) were used for this purpose. Both models were calibrated with experimental results for BRBs tested by Merritt, Uang, and Benzoni (2003) and Newell, Uang, and Benzoni (2006).

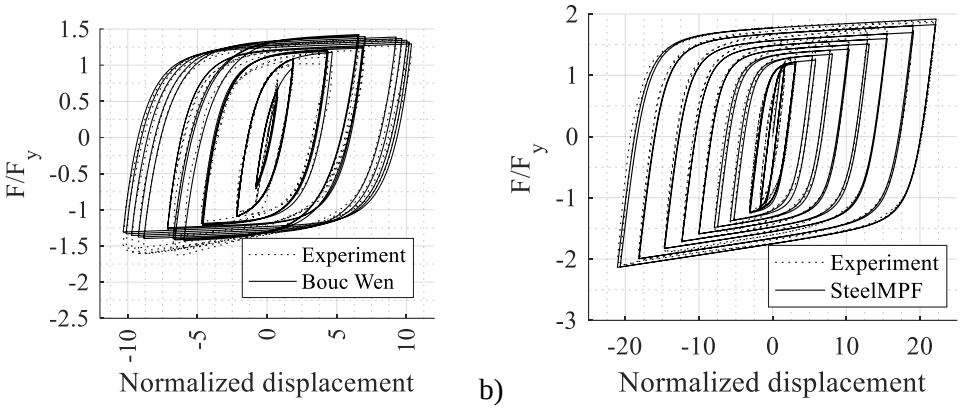

Figure 2-5 shows the resultant hysteretic loops of both models comparing with experimental results.

However, the introduction of isotropic hardening did not significantly reduce the concentration of ductility in the BRB connected to the abutment and those located at mid-length of the bridge. More specifically, the results from NL-RHA showed that there was a small reduction in the median ductility when the Bouc-Wen model was used, and almost the same response as before was obtained when the SteelMPF model was used. The reduction with the use of the Bouc-Wen model could be attributed to a small additional damping in the elastic range as this model does not have an initial linear range.

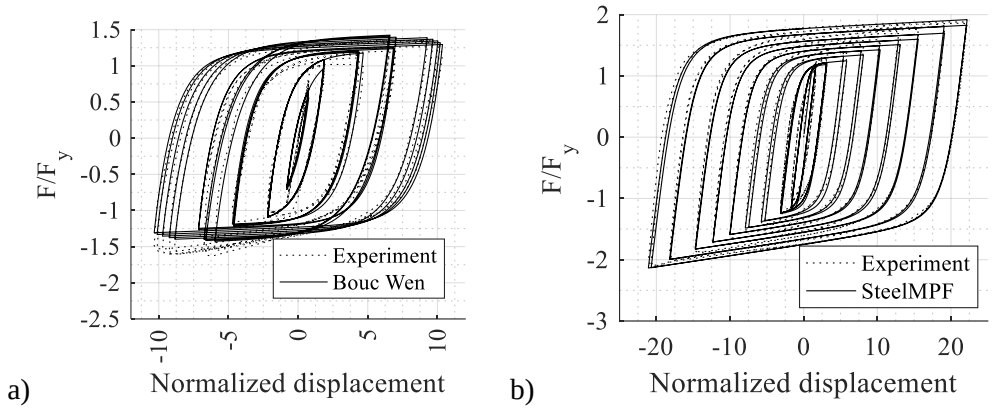

Figure 2-5 Adjusted models with isotropic hardening: a) Bouc Wen; b) SteelMPF

Another solution studied included increasing the post elastic stiffness in BRB. Increasing the post-elastic stiffness was artificial (as it could not necessarily be achieved without modifications of how BRBs are made), but it was done only to investigate the sensitivity of the results to this parameter. Post-stiffness ratios equal to 0.10, 0.2, and 0.3 were analyzed as tentative values for a bridge designed with R=5. Results showed that increasing post-elastic stiffness helps to better distribute ductility demands, as shown in Figure 2-6. However, the increase in the post-elastic stiffness also increases the force transmitted to piers. For instance, for a ductility equal to 4 and a post elastic stiffness equal to 0.3, the force transmitted would be close to 1.9 times the yield strength without considering strain hardening. Therefore, this option was discarded.

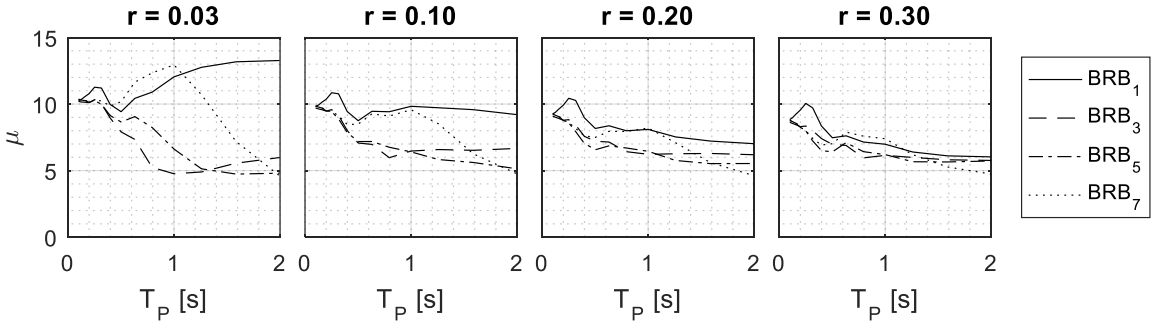

Figure 2-6 Median demand ductility of BRBs for a 7-span bridge designed based on RSA with different post-elastic stiffnesses (r) used in NL-RHA

Finally, a solution using of cables and allow pounding between spans was studied. Gap elements were used to model the distance between spans or between spans and abutments. Three options were considered: the first two assumed a maximum separation between spans of 5, and 10 times the yield displacement of the BRB, respectively, and; the third one assumed a maximum separation equal to 10 times the yield displacement but without cables or gaps between spans and the abutment. Results showed that when cables

are connected to the abutment, concentration in the ductility of BRBs connected to the abutment can be indeed improved; but when cables are not connected to abutments, similar ductility demands as to the case where cables are not used were obtained, as shown in Figure 2-7. Although the use of cables and gaps better distributed ductilities along the bridge, forces in cables in the order of 540 kips were developed, which would be difficult to transmit to the abutment.

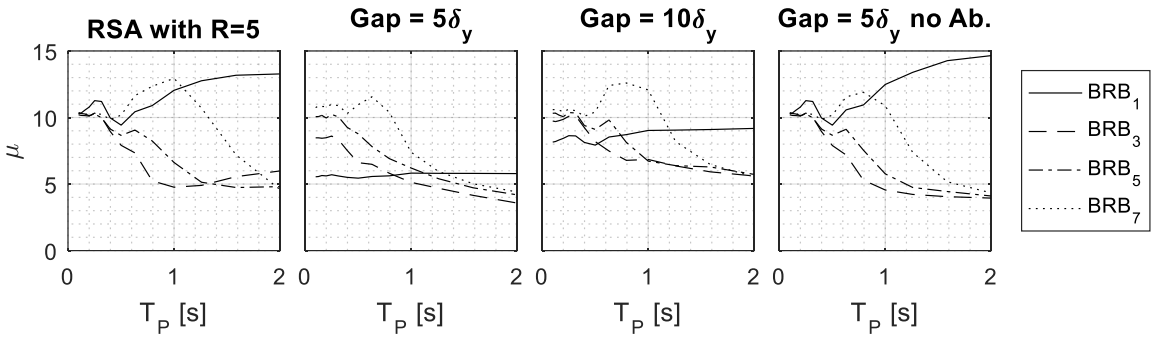

Figure 2-7 Median demand ductility of BRBs for a 7-span bridge: (a) without cables (reference model); (b) with cables and contact elements gap equal to $5\delta_y$; (c) with cables and contact elements gap equal to $10\delta_y$; (d) with cables and contact elements gap equal to $5\delta_y$ but no abutment

2.2.3 Seismic design based on nonlinear time history analysis – optimal design

As mention before, the design procedure based on RSA concentrates ductility demands in BRBs connected to abutments and BRBs located at mid-length of the bridge. Therefore, an optimization procedure and NL-RHA were used to determine the cross-section areas needed in each BRB along the entire bridge length such that the mean ductility demand (i.e., obtained from the 44 ground motions considered) is the same in each BRB. Initially, the target ductility demand was set equal to 5. Results obtained showed that the goal of uniform ductility demand in the BRBs along the bridge is achievable. To obtain an idea of an acceptable mean ductility demand, the research team contacted the Technical Director of Core Brace (Brandt Saxey) who suggested that a target ductility of 10 could be used since BRBs can easily accommodate this demand. For a target ductility equal to 10, bridges were designed considering three different BRB yield displacements (equal to 0.068", 0.138", and 0.276"), to investigate the influence of this parameter. Results showed that when smaller yield displacement were used, larger BRB cross-section areas were required (representing larger strength in the BRBs). This could be understood because the fundamental period of the structure reduces when shorter BRBs are used, usually resulting in higher spectral acceleration values, and eventually in the short period range, ductility demands greater than predicted by the "equal displacement theory." Results obtained from different yield displacements can also be interpreted as equivalent to results for bridges under different seismic hazard, where spectral accelerations shown in Figure 2-1 are multiplied

by factors equal to 2.0 and 0.5 (for bridges having BRBs with yield displacement equal to 0.068" and 0.276", respectively) with respect to the case of BRB yield displacement of 0.138". In this case, it is obvious that when the spectral acceleration increases, BRB cross-section areas increases.

2.2.4 Development of Equivalent Lateral Force (ELF) design procedure

It would greatly encourage implementation of ductile diaphragms if a simple procedure existed to design BRBs in the superstructure of bridges, making it possible for each BRB to ideally develop similar ductility demand along the length of the bridge. Therefore, based on results from the optimization procedure above, a design procedure similar in format to the Equivalent Lateral Force (ELF) design procedure used in buildings was proposed here. For reference, the distribution of forces along the height of buildings using the ELF procedure is based on the approximate mode shape of the first period and is defined as:

$$F_i = \frac{W\ Sa(T)}{R} \frac{m_i h_i^k}{\sum_{j=1}^{n_f} m_j h_j^k} \tag{3}$$

where F_i, m_i, and h_i are the lateral floor force, mass, and height of the i floor; n_f is the number of floors; W is the total mass; R is the reduction factor; $S_a(T)$ is the spectral acceleration at the fundamental period (T); and k is a factor that accounts for the influence of higher modes in the response of the structure and is a function of the period of the structure. The period of the structure is defined by empirical equations (such as those provided in ASCE-7). The R values for specific structural systems were defined based on past practice, but nowadays are determined by the FEMA P695 procedure for new structural systems.

The proposed ELF procedure for bridges with BRBs was developed by calibrating parameters to results from the optimal design approach based on NL-RHA. Recall that, at this point, regular bridges were studied where the mass of spans, pier stiffnesses, and length of each span do not change along the bridge. To apply the ELF procedure, a bridge with a given number of spans (N_{span}) is idealized based on normalized distance (x) which represent the position of the center of mass of each span along the bridge, which goes from zero at the mid-length of the bridge to ± 1 at the ends, and for the ith span is defined by Eq. (2). The influence of the stiffness of piers in the design was introduced with the parameter T_p, Eq. (1), which is defined as the period of one pier (calculated using the tributary mass from adjacent spans) and modeled as a SDOF. Some factors are calculated with Eq. (5) and are used later to define the properties of the structure. In these equations, T_{min} is the lower period that the structure can have, and it is achieved when piers are infinitely rigid. The mode shape, derived from optimal designs and curve fitted, is defined by Eq. (6) to (7), and is a function of the normalized distance (x) as well as the factors k_1 and k_2. The factors k_1 and k_2 are positive values which introduces the effect of higher modes and were fitted with Eq. (8) and (9), respectively. The

fundamental period (T) of the bridge is empirically defined by Eq. (10), which was the result of curve fitting of fundamental periods from the optimal design. Finally, the lateral force to be applied to each mass is calculated with Eq. (11), where m_i is the mass of the ith span, W is the total weight of the bridge, R is the response modification factor, and $Sa(T)$ is the spectral acceleration in units of gravity. Note that the format of Eq. (11) is similar to Eq. (3), as intended.

$$x = 1 - 2\frac{i-1}{N_{span}-1} \tag{4}$$

$$\gamma = \frac{T_p}{T_{min}} \tag{5.1}$$

$$\lambda = 1 - \frac{8}{\gamma^2 + 8} \tag{5.2}$$

$$\eta = \frac{T}{T_{min}} = 1 + 0.4 \cdot \lambda \cdot N_{span} \tag{5.3}$$

$$\phi(x, k_1, k_2) = 1 + y(x, k_1) - y(x, k_2) \tag{6}$$

$$y(x, k) = \left(0.6 + \frac{\mu}{100}\right) \cdot \left[1 - \frac{|x|^{\frac{1}{k}}}{1.1}\right]^k \tag{7}$$

$$k_1 = \min\left\{4 \cdot \lambda \ ; \ 0.15 \cdot (10 + \mu) \cdot \left[1 - 0.7^{(N_{mas}-2)}\right]\right\} > 0 \tag{8}$$

$$k_2 = 0.06(\gamma - 1) > 0 \tag{9}$$

$$T = \eta \cdot T_{min} \tag{10}$$

$$F_i = \frac{W\ Sa(T)}{R} \frac{m_i \phi(x_i)}{\sum_{j=1}^{N_{span}} m_j \phi(x_i)} \tag{11}$$

The minimum period of the structure (T_{min}) is the period of one span with its BRBs designed as a SDOF to reach a specific target ductility between 5 and 10. This can be achieved, using equations proposed for R values as a function of the ductility by different authors (Miranda and Bertero 1994, Riddell, Hidalgo, and Cruz 1989), or using displacement-based design (Priestley, Calvi, and Kowalsky 2007). Similar results are obtained with both methods with the difference that R-based design requires several iterations.

The R value was obtained by calculating the ratio between the force obtained multiplying the mass of the bridge by the spectral acceleration at the fundamental period of the bridge and the shear force required to reach yielding in the BRBs. It was observed that the reduction factor varies as a function of the number of spans and T_p, and it was defined by Eq. (12). Equation (12.1) was derived from the displacement amplification factor provided by AASHTO, Eq. (12.2) was fitted to consider ductility demands larger than

10, and Eq. (12.3) was fitted to include the effects of multi-degrees of freedom of the system and is equal to 1 for a SDOF system. Bridges with BRBs designed by the proposed ELF procedure were found to distribute ductility demands reasonably uniformly across all BRBs, with reduced concentration of ductility demands in individual BRBs.

$$R(T) = \begin{cases} \left(\frac{\mu}{\alpha_u \gamma_\mu} - 1\right)\frac{T}{1.25T_s} + 1 & if\ \ T < 1.25T_s \\ \frac{\mu}{\alpha_u \gamma_\mu} & otherwise \end{cases} \quad (12.1)$$

where

$$\alpha_u = 0.06\mu_{SDOF} + 0.7 \geq 1 \quad \text{if } \mu \leq 10 \quad (12.2)$$

$$\gamma_\mu = \frac{\mu_{max}}{\mu_{SDOF}} = 2\eta - 1 \leq 2.0 \quad (12.3)$$

2.2.5 Irregular bridges analyzed in the longitudinal direction

There can be an infinite number of different combinations of bridge mass variations from span to span, and of stiffness from pier to pier. Therefore, 210 bridges with random combinations of masses and spans were generated using Monte Carlo simulations for the case of bridges located over "single dip" valleys (or river profiles, for river crossings). For each realization of bridge configuration, the simulation began with the definition of the valley profile. The location of the lower point in the valley, relative to the length of the bridge, was selected randomly with a higher probability to be located in the central 40% of the bridge length. The depth of the valley, measured from the top of the deck, was also selected randomly and defined by the ratio between the maximum to the minimum depth. The resulting valley profile has the shape of an inverted Gaussian distribution, as shown in Figure 2-8. As a simplification, it was considered that all piers along the bridge have the same cross-section areas. Therefore, the stiffness of piers was only a function of the increase in pier height, assuming that piers were vertical cantilever elements fixed at their base. The maximum mass span along the bridge was defined randomly and located above the deepest point in the profile of the valley (as spans are typically expected to be longer where the height of piers is greater). The minimum mass spans were generically set equal to a specific value and the distribution of masses along the bridge was again defined by a Gaussian distribution, as shown in Figure 2-8 by the dashed line. Of all bridges so generated, maximum mass varied by a factor of up to three, maximum pier height ratio varied by a factor up to 2 (note that double the height of the pier in these examples corresponded to an eight times more flexible pier), and maximum mass and pier stiffness were not constrained to occur at the same time.

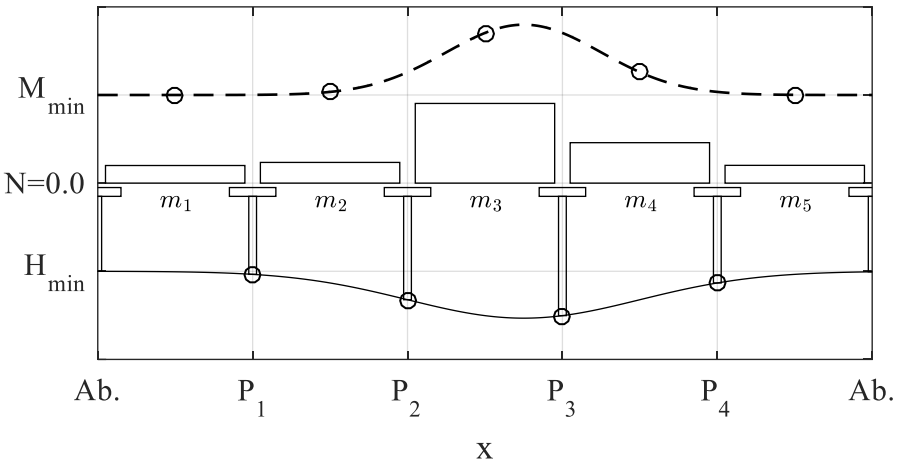

Figure 2-8 Determination of geometry using Monte Carlo Simulation

All bridges were designed with the ELF proposed procedure and analyzed with NL-RHA. Results revealed a concentration of BRB ductility demand in BRBs near the most flexible pier. This is because when piers are progressively more flexible than adjacent piers, the force demand in BRBs connecting to them reduces. To prevent extremely small areas, the BRB areas obtained using the ELF procedure was selected to be never less than half the BRB cross-section area calculated when piers are infinitely rigid. Ductility demand obtained with this minimum area constraint showed a better distribution than otherwise.

2.3 ANALYSIS OF REGULAR BRIDGES IN THE TRANSVERSE DIRECTION

Here, the set of regular bridges previously analyzed in the longitudinal direction was analyzed in the transverse direction. The difference with the longitudinal direction model is that, in the transverse direction, the rotational mass of the span was also considered. The rotational mass of a span depends on its geometry and, for rectangular bodies used to represent a span, in the aspect width-to-length ratio. The flexibility of span was not considered; i.e., for simplicity spans, were analyzed as rigid bodies. Two aspect ratios were selected, one equal to zero to approximate the case of bridges with long spans and few traffic lanes, and the second equal to one to represent the case of bridges with short spans and several traffic lanes. All models were designed based on RSA with constant R value equal to 5 and later analyzed with NL-RHA. Results for the cases with aspect ratio equal to zero showed that mean ductility demands in BRBs along the bridges are similar to each other, except for the BRBs connected to the abutments. The BRBs connected to abutments had up to 50% more demand in ductility than other BRBs when piers were relative stiff ($T_p < 0.7s$) and less ductility demand than the other BRBs when piers were more flexible (T_p>0.7s). Nevertheless, the mean demand ductilities ranged from 8 to 30. Similar behavior was observed when the span aspect ratio was set equal to 1. The difference was that, in that case, the mean ductility demands in BRBs connected to

abutments were closer to that of the other BRBs. Observation from bridges designed with RSA suggested that BRBs connected to each pier can be designed in the transversal direction as a simple degree of freedom system by considering half of the pier stiffness with one BRBs, the tributary mass from the adjacent spans, and half of the pier cap mass. Since the yield displacement and maximum elongation of BRBs are input values, displacement-based design was used, resulting in BRBs ductility demands close to the target value.

3 EXPERIMENTAL PHASE

3.1 OVERVIEW OF EXPERIMENTAL RESEARCH CONDUCTED

This second stage of the research program used shake table experiments to evaluate and validate the behavior of multi-span bridges having simply supported spans with bidirectional ductile end diaphragm equipped with BRB as the fuse element. More specifically, the testing program allowed to: evaluate different configurations of the bidirectional ductile end diaphragm; evaluate different types of connections between the BRBs and superstructure, and between the BRBs and concrete supports (i.e., abutments); evaluate the ability of these connections to allow the BRBs to perform as intended while accommodating the 3-D relative displacements that develop during the seismic response, and; evaluate experimentally obtained demand ductilities and compare them with results obtained from numerical analysis. Therefore, special attention was paid to the selection of a representative bridge prototype and the design of its corresponding scaled specimen. In this case, the specimen chosen represents the first span of the prototype bridge (i.e., connected to the abutment at one end and to a pier at the other).

3.1.1 Selection of the prototype and specimen

The objective of the bidirectional ductile end diaphragm is to limit superstructure displacements and dissipate seismic energy such that piers or bents remain elastic. Hence, a prototype was designed and analyzed to demonstrate that this behavior was achieved. Considering that the prototype and corresponding specimen are related by the laws of similitude (Harris and Sabnis 1999), design constraints were added to account for the fact that geometry, weight, and loads obtained from the prototype should be able to be replicated in the specimen within the limits of the testing facilities of the Structural Engineering and Earthquake Simulation Laboratory at the University at Buffalo. Therefore, after several analysis and design iterations to generate realistic and acceptable bridges geometries and ductile end diaphragms, the resulting prototype and specimen described below was obtained.

The prototype selected is a 5-span bridge with 100 ft long spans and bents heights varying from 16 ft to 18 ft (i.e. 10 to 12 ft columns plus 6ft height of the cap) as shown in Figure 3-1a and b. The superstructure of this bridge was designed in compliance with the AASHTO LRFD Bridge Design Specifications (2017). It consists of four built-up girders 66-3/4” deep, having 11”x1-5/8” flanges, and 5/8” web thickness; separated 15 ft between each other, and working as a composite section with a 9-1/8” thick concrete slab. The final weight of the span was estimated equal to 972 kips. Spans are supported on bents, each having three 54”x48” columns with equal height, as shown in Figure 3-1b.

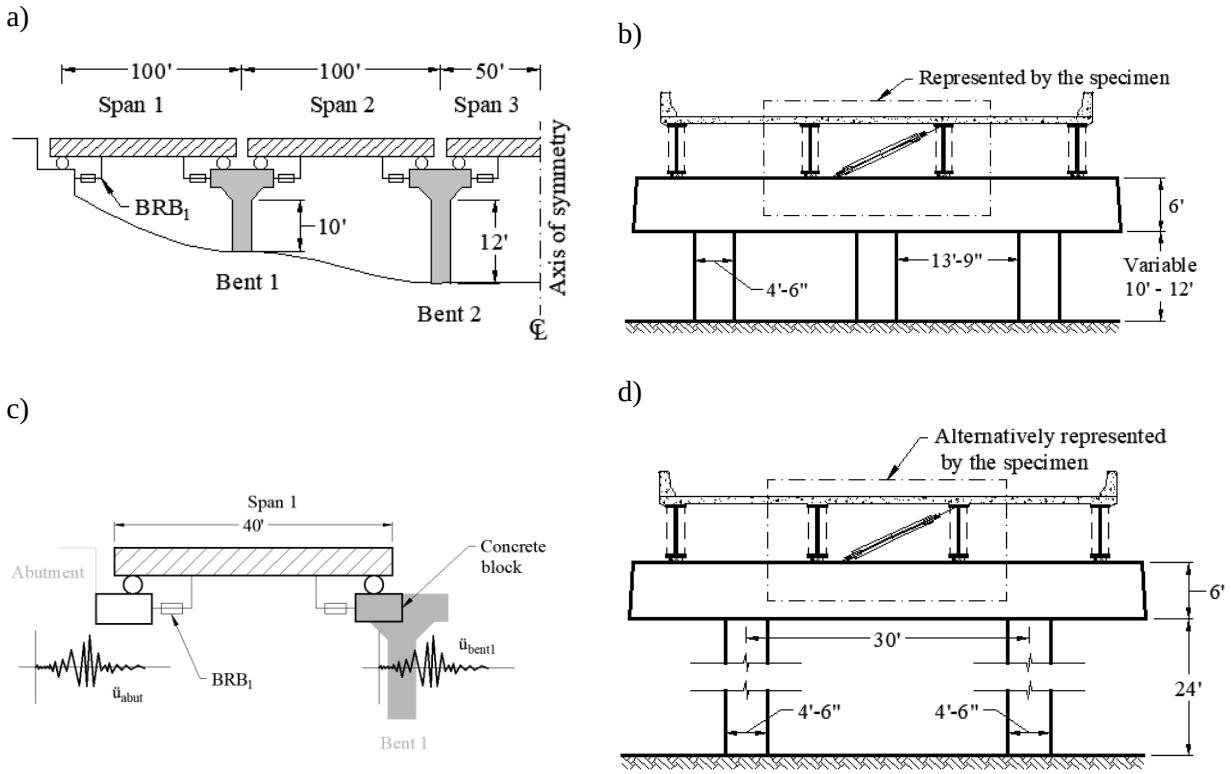

Figure 3-1 Prototype: a) scheme in the longitudinal direction, b) geometry in the transversal direction

From this prototype, the specimen to be tested has a scale of 1/2.5 and assumes a model with a 1.0 factor for gravity scaling. The specimen represents Span 1 in Figure 3-1a, where only the part of the superstructure with the ductile end diaphragm and its connection to concrete is modeled, as shown in Figure 3-1b. Girders in the specimen are W27x84 shape, with a 26.7" depth, spaced 6 ft (per direct scaling of the girder depth and spacing in the prototype). The bent cap and abutment are represented by concrete blocks, each one of them connected to a different shake table. The shake tables reproduced scaled acceleration and displacement histories obtained from the analytical model at the bent cap and abutment, respectively. A schematic of this concept for the specimen is shown in Figure 3-1c, where the abutment is the west shake table and the pier cap is the east shake table.

The yielding core areas of the BRBs were determined using the simplified designs method described earlier. In applying this procedure, for calculating stiffness, bents were assumed as cantilever columns (fixed at their base) in the longitudinal direction, and; in the transverse direction, bent caps and foundation were considered as rigid. Furthermore, the design spectrum was the one shown in Figure 2-1 reduced by a factor of 1.28. As a result, in the specimen, BRBs in the transverse direction require a cross-section area equal to

0.5 in², and; in the longitudinal direction 0.84 in² and 0.54 in² for BRBs connected to the abutment and to the bent cap, respectively. Note that 0.5 in² was considered here to be the smallest cross-section area that can be manufactured to have a good performance in a cyclic test.

Notice that short bents in the bridge prototype were selected to meet the two experimental constraints that: (i) the BRBs in the specimen needed to have a yielding cross-section area of at least 0.5 in², and; (ii) accelerations obtained at the top of the bent cap (for the set of ground motions scaled to the design spectrum) needed to smaller than the maximum acceleration that can be provided by the shake table. Nevertheless, a bridge with taller bents, shown in Figure 3-1d, was also analyzed as a candidate for prototype. It also showed good performance of the ductile end diaphragms with BRBs designed per the simplified methods, but was not selected for testing because accelerations at the pier cap level were larger than could be applied by the shake table. In both bridges, the superstructure was the same as described above.

3.1.2 BRB configurations

BRBs in bidirectional ductile end diaphragm and connecting the superstructure with the substructure can be provided in different configurations as long as the strength and stiffness provided by the group of BRBs in the longitudinal and transverse directions are in compliance with the design requirements. This provides for much flexibility in design and detailing. For that reason, two BRB configurations for the prototype bridges were analyzed and considered as possible candidates to be used in the specimen to be tested.

Both configurations recommended for the experimental program considered one end of the BRB connected to the abutment or bent cap while the other end was connected to the superstructure. The first configuration (named Configuration I here) considers a BRB in the transverse direction that connects to the superstructure at a point close to the top flange of the girder, while BRBs in the longitudinal direction are installed horizontally, as shown in Figure 3-3a. The advantage of this configuration is that forces in the end cross-frames are small, as cross-frames are only required to prevent lateral-torsional-bucking of the girders during construction. The second configuration tested (called Configuration II) is a modified version of Configuration I where the longitudinal BRBs are connected close to the top flange of the girder, as shown in Figure 3-3b. The advantage of this configuration is that the BRBs in the longitudinal direction are nested between the girders and thus protected from possible vehicle impacts. In both configurations, connections of slanted BRBs are subjected to rotations about two orthogonal axes.

a) 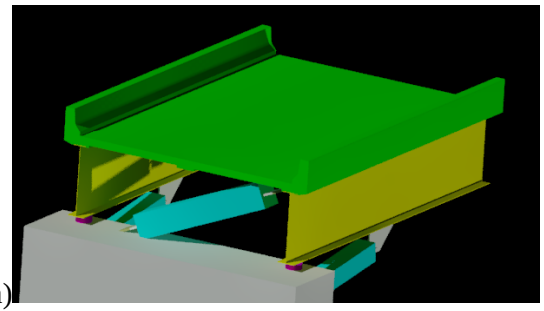 b) 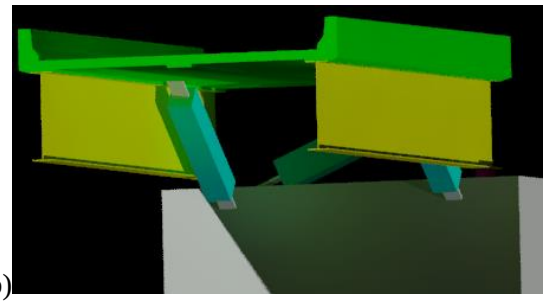

Figure 3-2 Sketch of BRB configurations: a) Configuration I, and b) Configuration II

3.1.3 Connection of BRB-to-girder

In some cases, connections of BRBs used in bidirectional ductile diaphragms may have special requirements compared with the connections typically used for BRBs in braced frames. This is because the connection used with BRBs in some of the configurations considered here must be able to allow rotation in two orthogonal directions. For instance, for the BRB shown in Figure 3-3, the local axes in the connection (where all axes are perpendicular to each other) can be defined as: *y* is parallel to the longitudinal axis of the brace, *z* is in the vertical plane at the end of the span (plane shown in Figure 3-3), and *x* is parallel to the longitudinal direction of the bridge (normal to the plane shown in Figure 3-3). BRB connection rotations generated in a seismic event are expected to develop around the axis *x* and *z* when the span moves in the transverse and longitudinal direction, respectively.

To address rotation in two orthogonal directions, four types of BRB connections were considered to be used in the experiment. One of them was previously tested by Wei and Bruneau (2016), one was used previously in the seismic retrofit of Vancouver's city hall and featured on a CoreBrace web page (2020), one was a standard pinned connection featured on a CoreBrace web page (2020), and one was developed and proposed by the authors. The connection used by Wei and Bruneau is pinned in the *x* direction, while in the *z* direction it relies on the elastic deformation of BRB end plates, as shown in Figure 3-4a. The detail of the connection used in the Vancouver city hall could provide rotation around z axis by plastic bending of the gusset plate (in the shaded area shown Figure 3-4b), and around the *x* direction by elastic bending of end plates in their strong axis or due to bolt slippage; alternatively, the set of bolts could be substituted by a single pin, as shown in Figure 3-4c. The fourth connection, shown in Figure 3-4d and referred to here as a "universal connection", resulted from the merging of two connection concepts that have been previously used in concentrically braced frames, such as to provide rotational capacity by plastic bending in the red shaded areas shown in Figure 3-4d. This connection is made by using a gusset plate orthogonal to the end plate from the BRB. For the detail shown in the figure, both plates are welded; however, a bolted connection option with four angles was proposed instead for easier BRB replacement during the testing program.

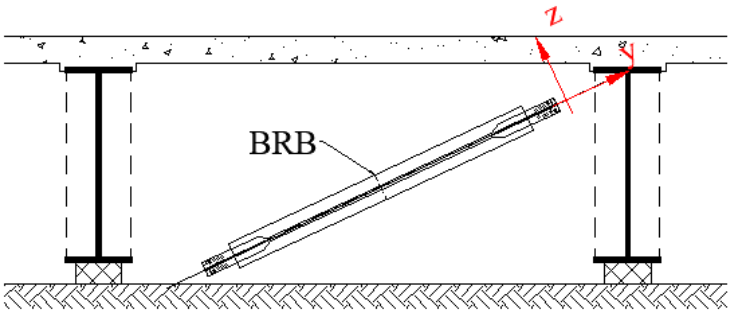

Figure 3-3 Rotations in BRB-to-girder connection in transverse direction

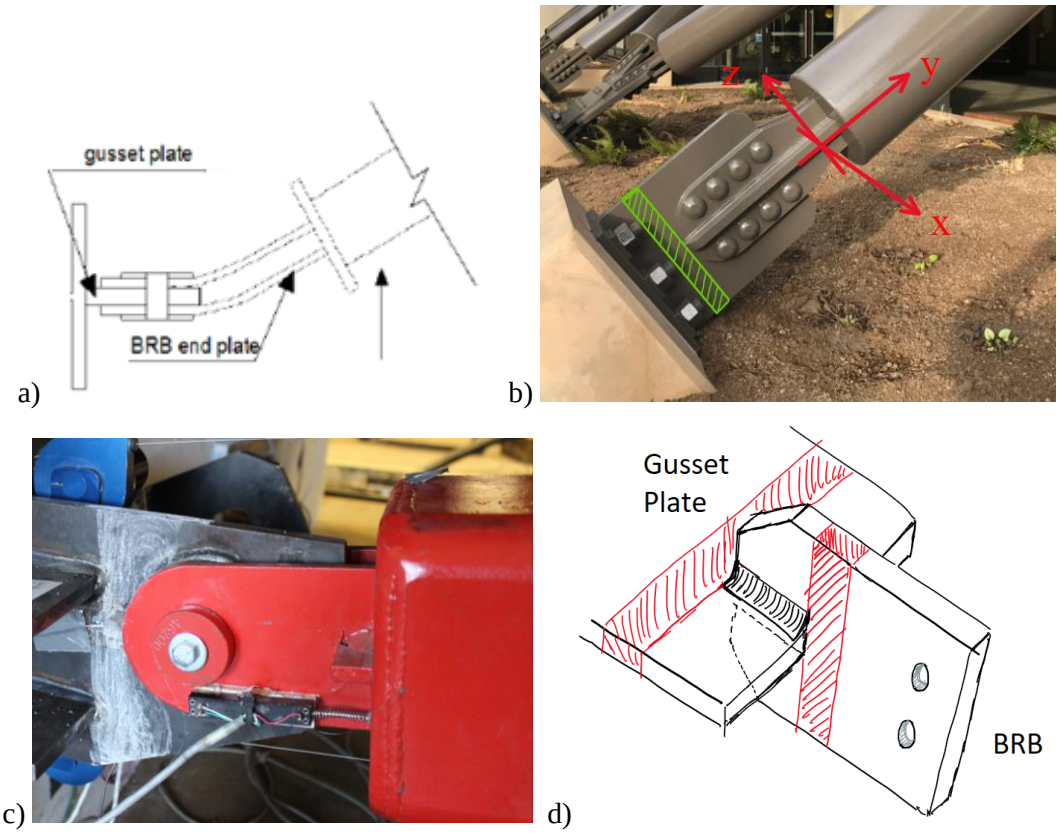

Figure 3-4 BRB-to-girder connections: a) with flexure in end plates (Wei and Bruneau 2016), b) with bolted connection (CoreBrace 2020), c) with bolted connection (CoreBrace 2020), and d) universal connection

3.1.4 Connection of BRB to concrete

This section presents details on different connection concepts that were used to transfers forces from the BRBs to the span supports (e.g., abutment or bent cap). Moreover, since bidirectional ductile end diaphragms can be implemented both in existing bridges and in new bridges, here, connections that can be either post-installed or cast-in place in concrete were both studied. Initially, connections with a base plate and post installed anchors using injectable adhesive were analyzed as a possible solution, but it was found that this strategy required an inordinately large number of anchors and considerable space for the case of BRBs in the longitudinal direction (because they transfer large tensile forces), so it was deemed to be unpractical for those BRBs. Instead, this concept was considered for the case of BRBs in the transverse direction since the tensile force transferred through the connection is the smallest. Since this connection uses post installed elements, it could be used as a retrofit solution. Additionally, three other connection configurations were studied: one for retrofitting and two for new construction. The first uses a base plate with an 8" long, 1.5" wide, and 0.75" thick shear lug connected with four 3/4" diameter rods, F1554 Grade 36 steel, and pretensioned to an anchor plate on the back concrete face, as shown in Figure 3-5a. The second one uses a base plate with the same shear lug as described before and six 3/4" diameter J-hooked bolts, F1554 Grade 36 steel, pretensioned, and embedded in the concrete, as shown in Figure 3-5b. A variation to this connection, shown in Figure 3-5c, uses four 3/4" diameter J-hooked bolts, F1554 Grade 36 steel, pretensioned, embedded in the concrete over the length required for development of the hook, and with additional stirrups to ensure anchorage. The third one uses an embedded W10x19 steel shape with studs welded in the flanges as shown in Figure 3-5d. Slight modifications to the presented concepts were used for the different BRBs in the two configurations. In total 6 different connections between BRBs and concrete blocks (the substructure) were used in testing.

3.1.5 Design of load transfer from slab to BRB

The inertia forces generated in the bridge superstructure in a seismic event mainly comes from the mass of the concrete deck. In the transverse direction, that force needs to be transferred to the ductile end diaphragms to be resisted by the BRBs. An adequate load path from the slab to the diaphragm must therefore be established. Here, a steel element with welded shear studs was designed to transfer an inertia force equal to (per capacity design principles) yielding and strain hardening of the BRBs of the ductile end diaphragms. In each end diaphragm, 11 studs 3/8" diameters and 2 1/8" long were designed to be welded along the flange of a T2.5x9.5 shape located between girders in the transverse end diaphragm, as shown in Figure 3-6. Note that this detail is similar to one that has been developed by Carden, Itani, and Buckle (2008).

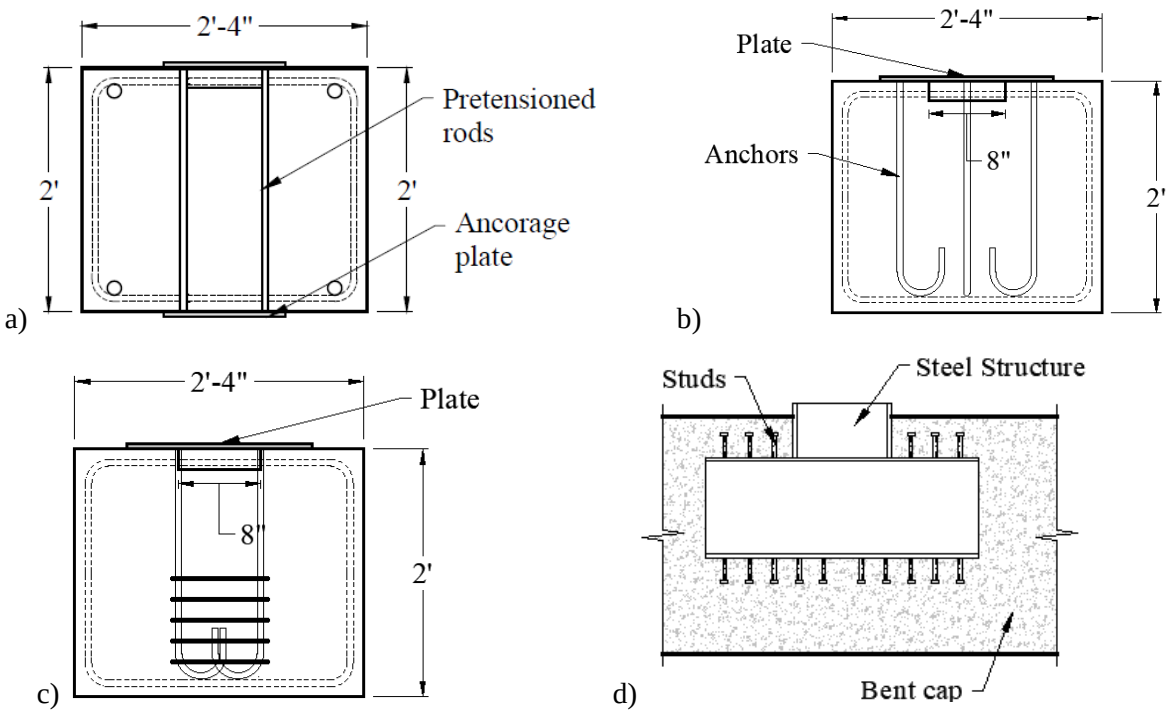

Figure 3-5 Connection to concrete with a) pretensioned rods, b) J-hooked anchors, c) J-hooked anchors with stirrups, and d) embedded steel shape

In the longitudinal direction, forces from the concrete deck need to be transferred to the girder to be later be resisted by BRBs. Here, similar to what was done in the transverse direction, capacity design was used to design studs welded on the girders of the specimen to directly transfer this inertia forces from the slab to the girders, to ensure yielding in the BRBs connected to girders. In each girder, 16 studs 3/8" diameters and 2-1/8" long were designed, to be welded equally spaced along the span.

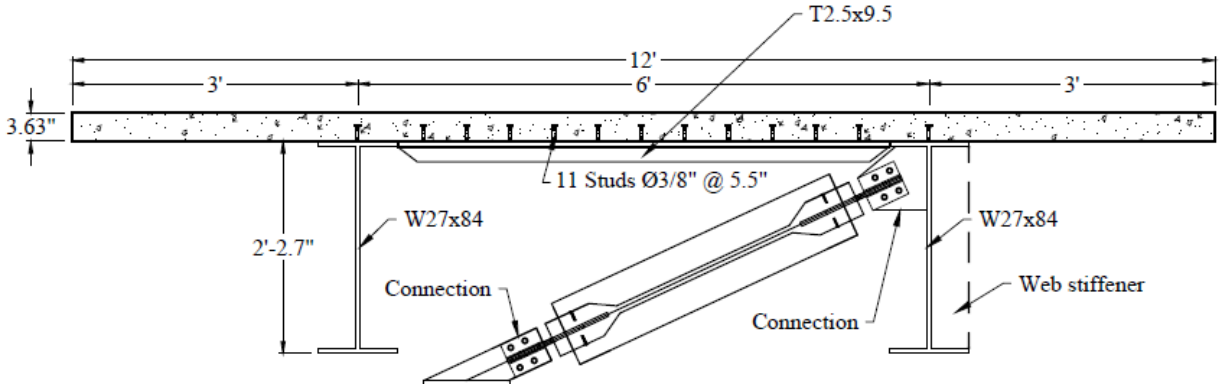

Figure 3-6 Studs in the transverse end diaphragm

3.1.6 Cross-frames

Intermediate and end cross-frames are designed to transfer lateral forces to abutments or piers. In the case of seismic forces, Zahrai and Bruneau (1998) demonstrated numerically that intermediate cross-frames do not contribute significantly to the seismic behavior of slab-on-girder bridges, but that end cross-frames are important parts of the seismic load path in such structures. Here, since BRBs connected at end diaphragms take care of resisting the seismic forces, cross-frames are only needed to brace the girders and avoid instabilities at the construction stage. AASHTO does not provide forces to design these elements; therefore, requirements for lateral bracing taken from AISC 360 (2016) were used to design these cross-frames. The resulting cross-frames have two diagonals in an "X" configuration and a horizontal element located as shown in Figure 3-7. Diagonals are connected at each end to web stiffeners with two 5/8" diameter bolts, and are connected to each other at their intersection point with one 5/8" diameter bolt. The horizontal element is connected with 2 bolts at each end to the girder web stiffeners. All braces are L2x2x1/4 shapes and spaced 10 ft between each other, which corresponds to the 25 ft spacing in the prototype recommended in previous editions of AASHTO LRFD.

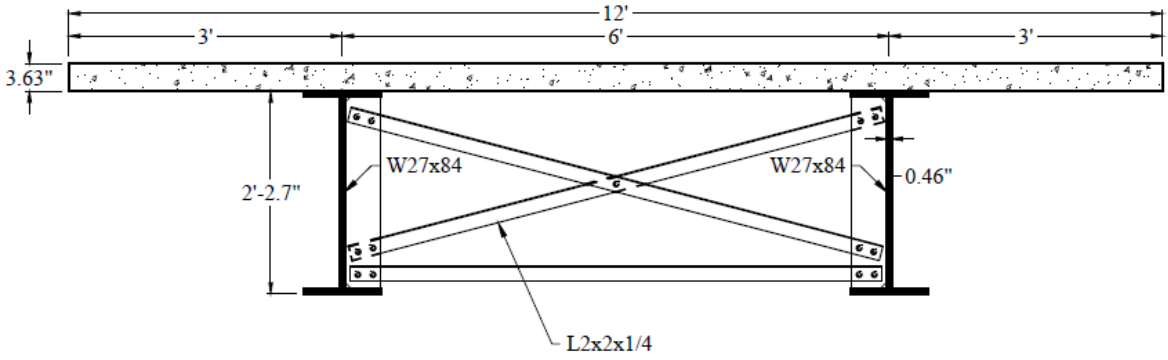

Figure 3-7 Detail of cross-frames

3.1.7 Specimen Design Process

In the experiment, BRBs were expected to act as fuse elements dissipating seismic energy and avoiding damage in the remain structure. To achieve this behavior all components were designed based on plastic analysis and capacity design principles considering that BRBs reach their maximum probable force. The components defined are:

- Connections between BRBs and base plate,
- Connection between base plates to foundation
- Connection between BRB to girders
- Bearings and connection to foundation and girder
- Concrete foundation

- Connection of foundation to shake table
- Failure protection system (as safety measures to protect equipment)

This process required several iterations including checking of constructability issues. This design process is described in the flowchart shown in Figure 3-8.

The bridge specimen was designed up to a 60% level, after which feedback was collected from the BRB and bearing manufacturers to be able to progress further. The factors used in this capacity design and that considers hardening of the element were provided by CoreBrace. However, these factors were only approximate, for preliminary design purposes, since actual values were unknown for the BRBs at the scale of the test, and were to be confirmed by testing. Different details were used for different configurations of BRBs; however, all were implemented in a common deck as shown in Figure 3-9. Preliminary details were shared with High Steel (https://www.highsteel.com/), a steel fabricator identified by AISC. Detailing recommendations were implemented (e.g., minimum welding filled was increased to 1/4"). Final design was modified as required due to changes in geometry of the BRBs and bearings provided by suppliers.

3.1.8 Simulation of the shake table test

Using the specimen geometry obtained in Section 3.1.1, a detailed computer model was created to simulate the shake table test. Figure 3-10 shows a 3D view of the test specimen with the concrete block to be attached to the shake table shown in orange, and a deformed shape of the detailed model. Note that the specimen was supported by two shake tables, one at each end. One shake table represented the abutment and the other the cap of a pier; hence, shake tables excitations were unsynchronized. The study included the generation of input excitation for the shake table. The simulation confirmed that using unsynchronized tables generated inertia forces in the specimen adequate and representative for the expected dynamic test.

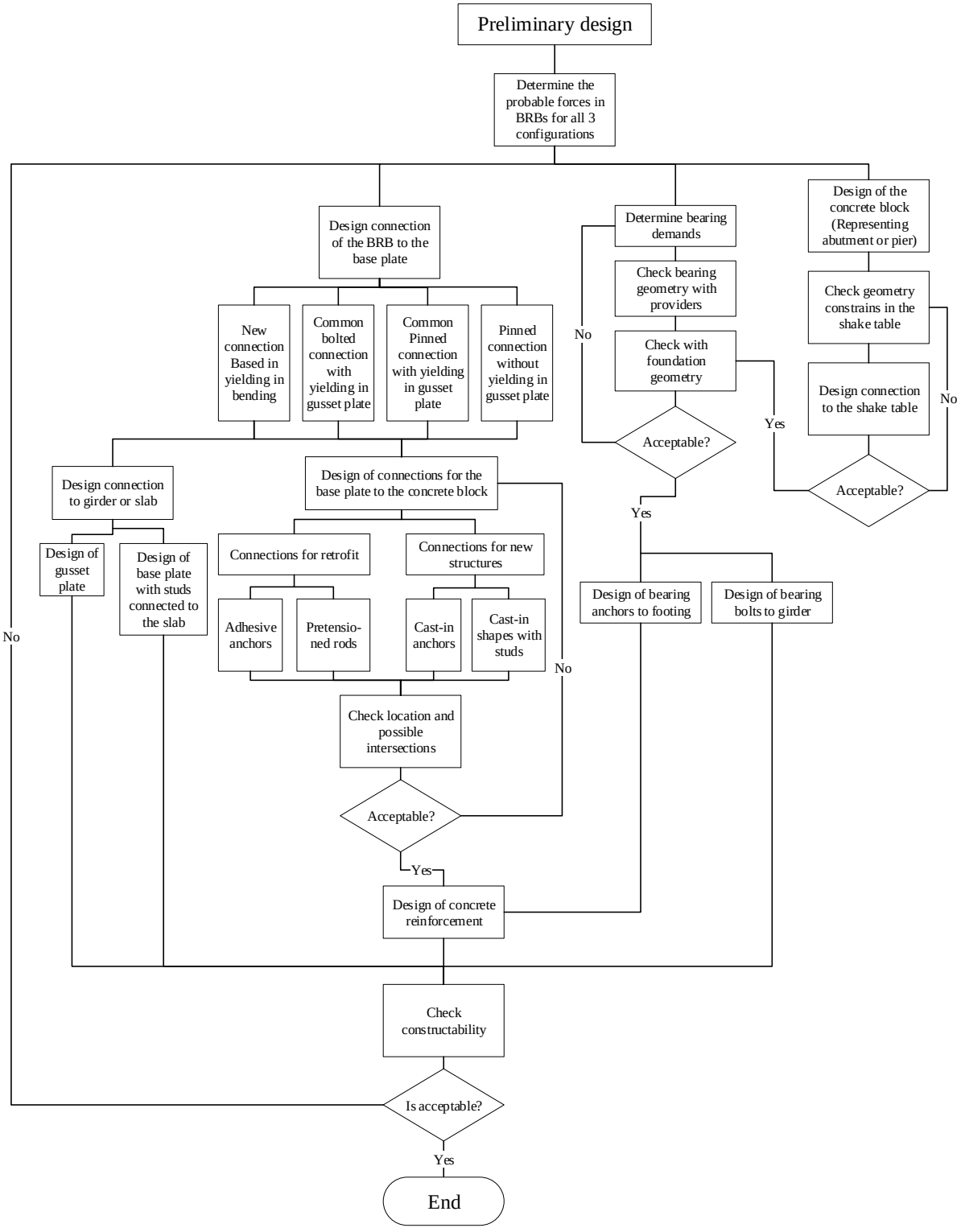

Figure 3-8: Design flow chart

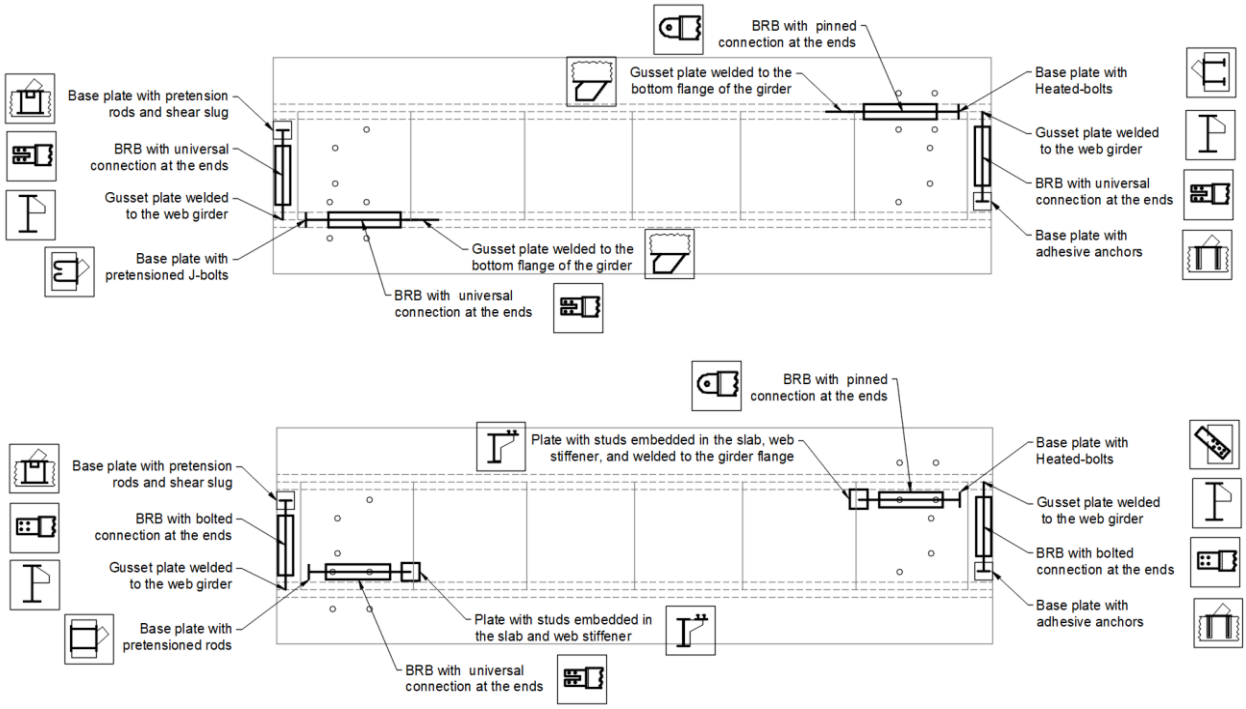

Figure 3-9: Location of different details in plan view of bridge specimen

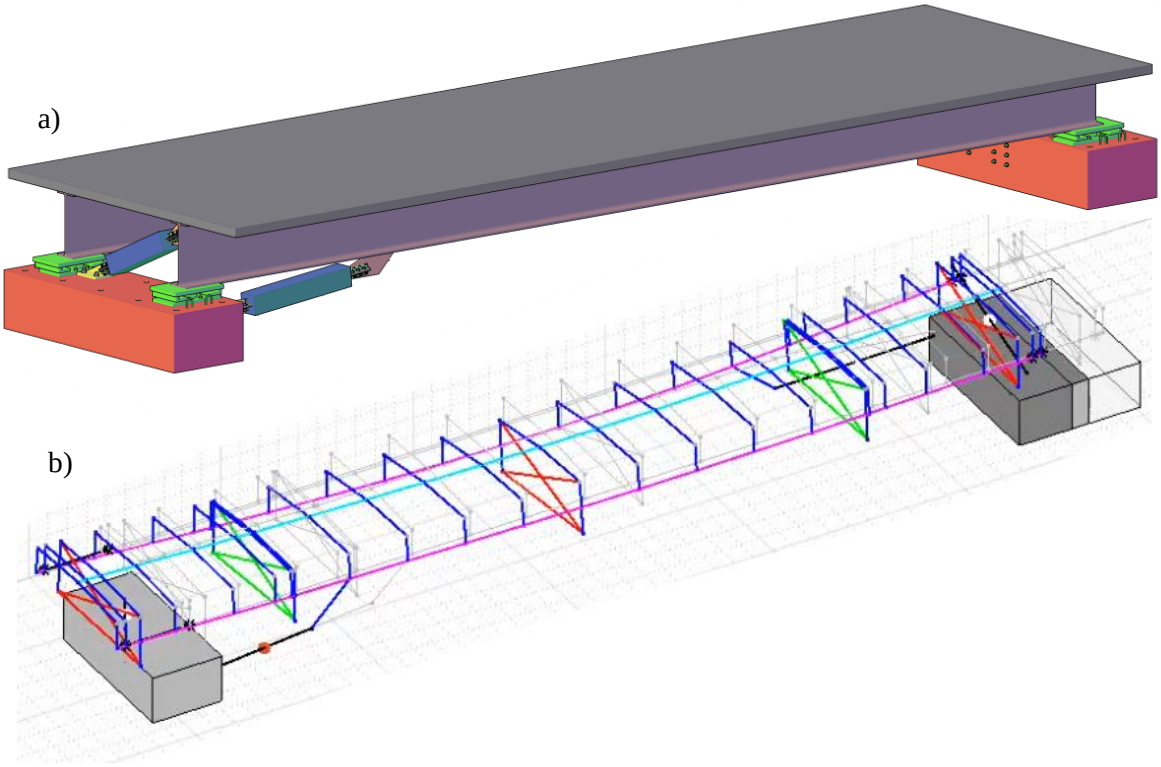

Figure 3-10: Specimen: a) 3D view; b) deformed shape of the detailed model

3.1.9 BRB testing and design

From the preliminary design, the BRB length, the geometry of the BRB end connections, BRB strength, and BRB yield displacements were defined and shared with CoreBrace, which was responsible for designing and detailing the BRBs (e.g., yielding core, transition zone, size of casing, etc.). However, for the scaled specimen, the length of the BRB and the strength were smaller than what is typical for BRBs used in construction. Reaching those small strengths required yielding core areas close to 0.5 in² and the use of steel with a low yield stress. To ensure the adequate behavior of a BRB with such a small area (never tested by CoreBrace before) and to obtain the strain hardening parameters needed for capacity design of the rest of the structure, two BRBs were designed and shipped to the University of Buffalo where they were tested. The BRB set-up is shown in Figure 3-11. A 3d view of the test set-up is shown in Figure 3-12.

The BRBs had 0.5 in² of cross-section area and an expected yielding strength equal to 19.05 kips. The expected yield displacement, Δ_y, of the BRB was 0.0256 in. With this yield displacement, the testing protocol was defined following AISC 341 for a design displacement equal to 0.256 in (10 Δ_y). After reaching a displacement equal to 20 Δ_y, different cycle amplitudes were used to complete each BRB test. For the first BRB, cycles were applied up to a ductility equal to 25 Δ_y. Two complete cycles were completed before the yielding core broke in tension. For the second BRB, several cycles with an amplitude equal to 20 Δ_y were applied until the failure of the BRB.

As a result of the BRB testing, the strain hardening of the core was obtained for different displacement amplitudes. Backbones curves for each BRB test and the average curve are shown in Figure 3-13. These curves were used by CoreBrace for the design of the BRBs for the shake table testing program. In the updated design process, some BRBs yield displacements had to be modified since there was not enough length inside the casing to accommodate the transition zone needed to ensure satisfactory behavior. Taking these changes into account, BRBs design was finalized and drawings were released for production. In production, by error, only half of the BRBs were fabricated. The error was discovered prior to shipping. As a result, a second set of BRBs were produced and shipped to the UB SEESL in a separate batch. The BRBs in that second batch were stronger than the first ones because those BRBs were produced with a plate having a higher yield strength.

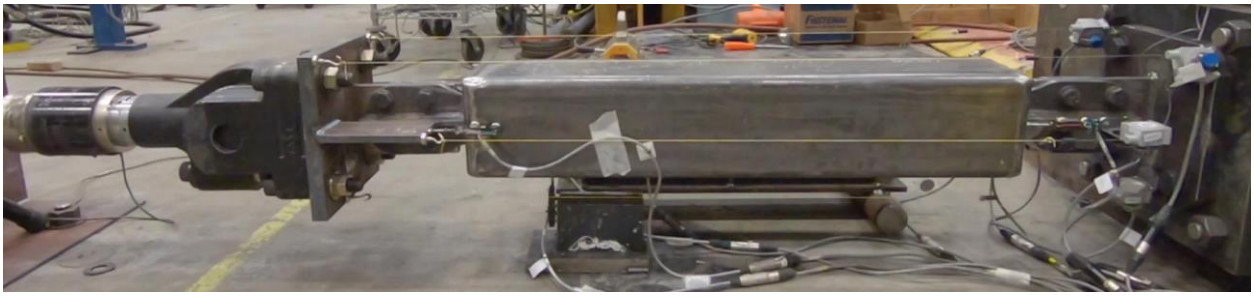

Figure 3-11: BRB axial test set-up

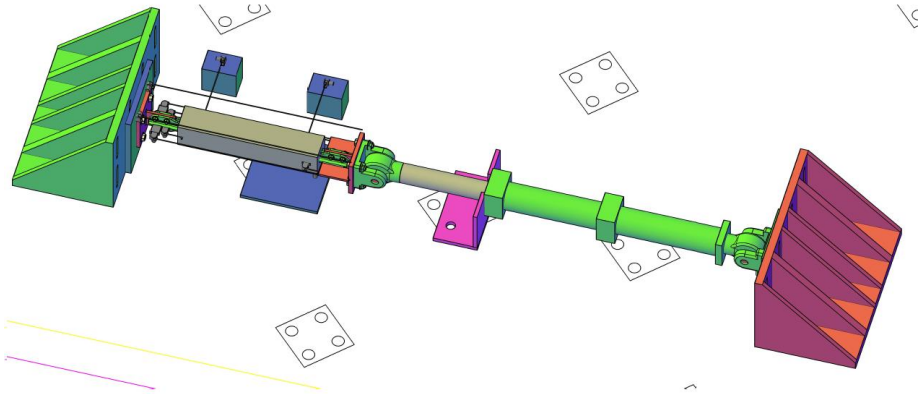

Figure 3-12: conceptual view of BRB axial test set-up

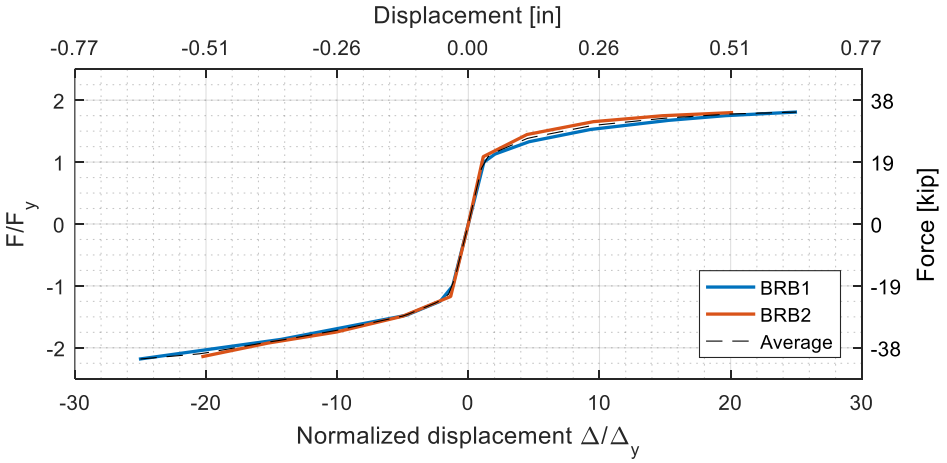

Figure 3-13: BRB Backbone curve

3.1.10 Bearing design

Initially, bearings were preliminary sized based on the expected demand. The sizing was coordinated with RJ Watson (the bearing supplier for this project), and was used for the design and location of details in the concrete blocks. Once the geometry was accepted, RJ Watson finalized the design of the bearings and submitted the final drawings for approval. A lateral view of the bearing is shown in Figure 3-14. Drawings

were approved and submitted for manufacturing. A byproduct of the final design was an increase in height of the bearing, which requires modification of all the BRB connection details accordingly.

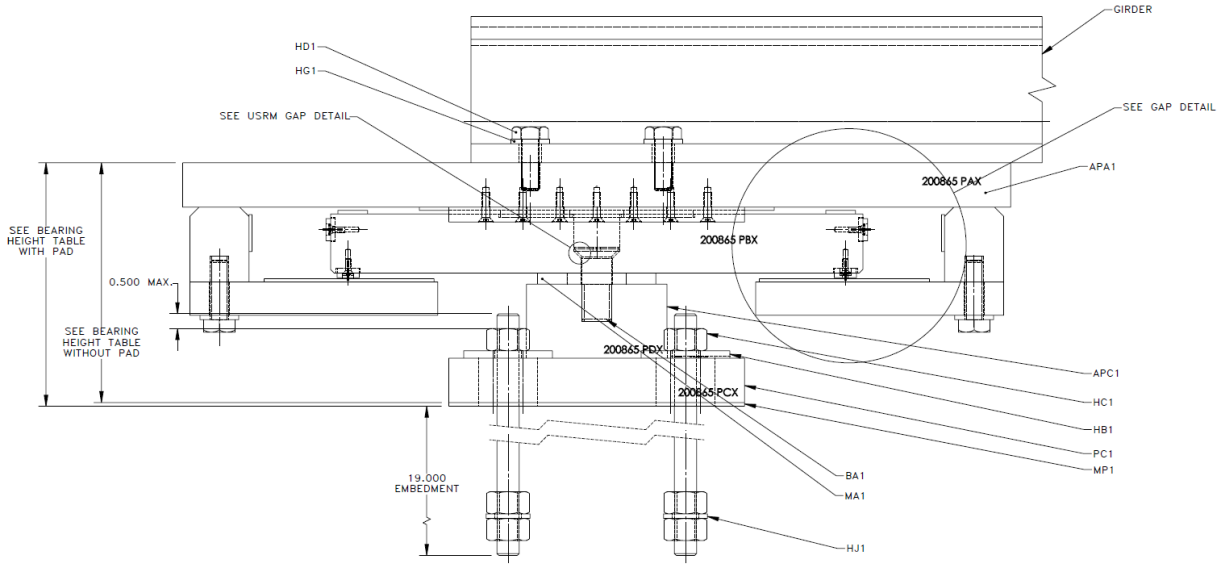

Figure 3-14: Bearing lateral view

After the bearings were manufactured, the bearings were tested under static loads (at small velocities) to verify their friction coefficient and ensure that the force taken by bearings was small enough to be negligible (as it was indeed neglected during design of the specimens). Note that the bearings were also designed to provide an uplifting resistance that was required to resist tension forces at the support resulting from the specific layout of BRBs in the specimen and the reduction in mass resulting from the scaling process. Therefore, bearings were tested under compression and tension at the R.J. Watson facilities. Figure 3 shows the set-up for both tests. The resulting friction coefficients obtained were 0.008 and 0.09 in compression and tension, respectively, with the coefficient in tension being effectively an order of magnitude greater than in compression. For the friction coefficient in compression and the weight of the specimen (63 kips), the corresponding lateral load needed to initiate sliding at each support (i.e. abutment or pier) was 0.25 kips. Comparing this with the horizontal projection of the yielding force of the weakest BRB (16.8 kips), the friction force in each support was 1.5 % of the BRB strength. Hence, this confirmed that the assumption of neglecting the friction force developed by the bearings during the design was correct. Finally, bearings were shipped to the UB SEESL laboratory where they were stored while awaiting shake table testing of the specimen.

a)  b) 

Figure 3: Bearing test set up: a) compression, b) tension

3.1.11 Final design and steel fabrication

With bearings and BRBs designs finalized, the design of connections and their detailing were finalized. Drawings were also finalized and shared with the steel fabrication. Drawings were reviewed and some additional information regarding details was required. After corrections, drawings were released for fabrication. However, a COVID-19 related labor shortage significantly delayed the process. Fabrication of the specimen finally began in early September 2021. Progress was slow, again due to challenges associated with COVID-19. To continuously obtain updated status of fabrication, in addition to an initial in-person inspection, several virtual inspections of the steel structure were performed. The virtual inspection was based on videos that showed different views of the specimen. Figure 3-15 shows a frame of on such video with annotations pointing to a discrepancy (which was consequently fixed) between the fabricated structure compared with details in drawings. The steel structure was finalized and accepted by mid-December 2021. By the end of December 2021, the steel structure was shipped to High Concrete where the slab was poured. Finally, the deck was delivered on February 7th 2022 at UB SEESL.

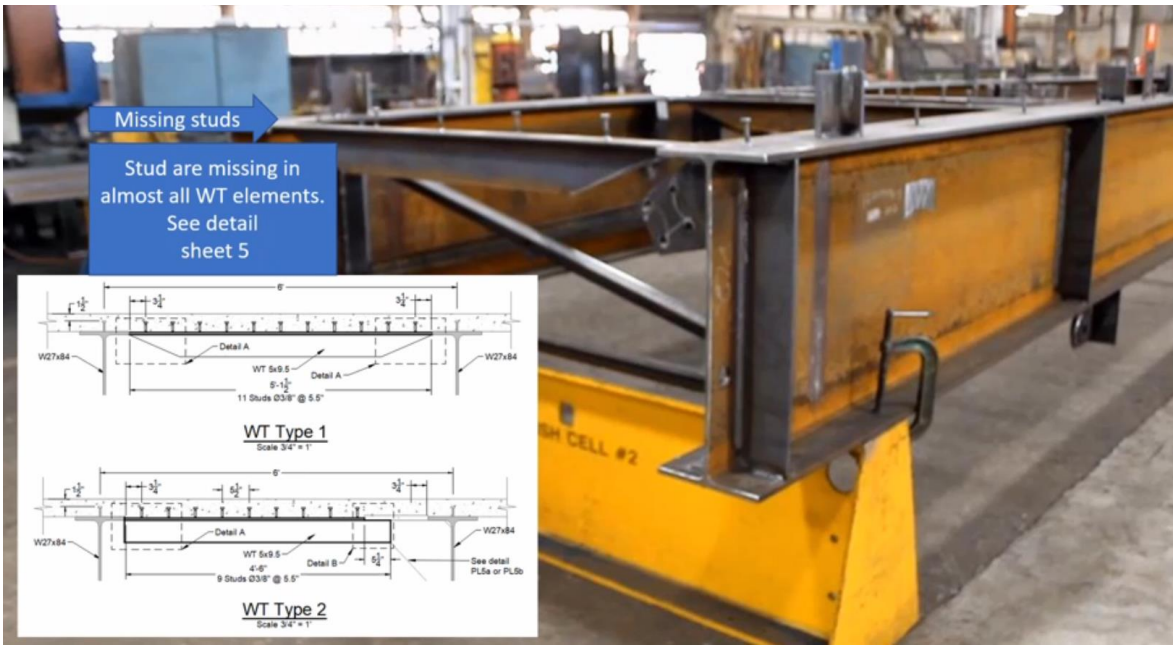

Figure 3-15: Example of virtual inspection

3.1.12 Instrumentation plan

During testing, collecting data from the BRBs was one of the most important tasks. Therefore, since the BRB yield displacements are small (~0.03 in), 4 Linear Potentiometers (LP) were used in each BRB to measure the displacement of BRBs, two at each end. Additionally, each BRB had 2 String Potentiometers (SP) to measure large displacements between the gusset plates where BRBs were connected, and 2 to 6 Strain Gauges (SG) were installed on the BRB endplates to measure axial and bending strains in the endplates and used to also monitor the integrity of the BRB (i.e., its ability to resist axial forces). A minimum of 8 instruments were used per BRB. For the remaining structure; several SP, LP, SG, and accelerometers were used to provide a relatively comprehensive measurement of its behavior. A total of 156 instruments were used. As an example, Figure 3-16 shows the location of SP attached to the slab.

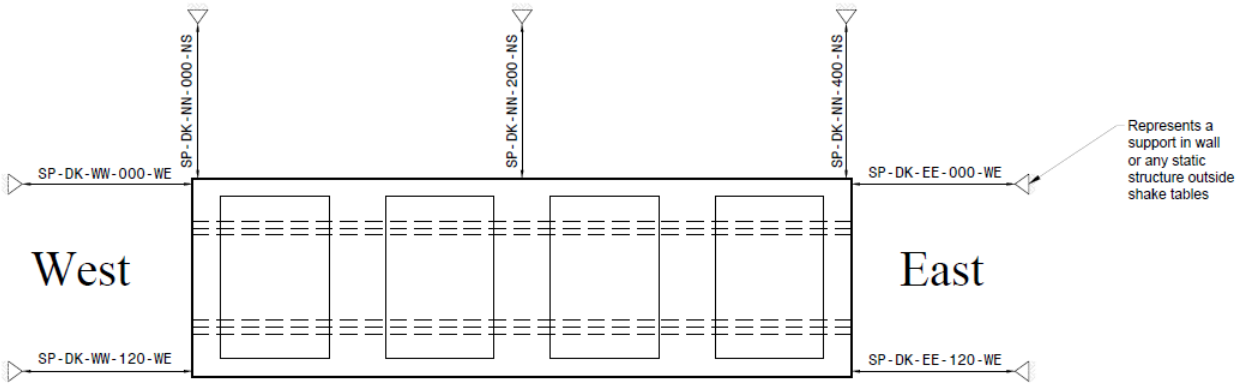

Figure 3-16: String pots attached to the slab

3.1.13 Selection of motion histories

To obtain ground motions representative of the design level, four long-duration and strong ground motions were selected to be used as seeds for the spectral matching process. For scaling, the original design spectrum was adjusted such that the strength of BRBs required per the design procedure proposed in Stage 1 was similar to the strength of the BRBs delivered to SEESL. Additionally, five motions were selected and amplitude-scaled to generate the largest possible displacement demands in the BRBs. These motions were representative of near-fault motions, far-field motions, motions with pulses, and motions in soft soils. Finally, as a contingency in case the BRBs could not be failed under the previous motions, two extreme motions were selected and used as the input of both shake tables, representing the case of stiff piers. All the final motion histories were scaled in time and amplitude to be used with the specimen. Then, the motions were exported in a format useful for the shake table control system.

The motion used to represent thermal expansion was obtained from the numerical model of the prototype subject to 75 years of temperature variations. The temperature record from Memphis was used as the input. For this sequence, one table was kept fixed while the other shake table moved in the longitudinal direction.

3.2 TESTING

The specimen setup had four different BRBs per configuration and was subject to: 1) a sequence of thermal expansion demands to represent their respective life-cycle demands, 2) a sequence of four spectral matched earthquake displacement histories (with components in the longitudinal and transverse direction of the bridge) that represents the design level, 3) a sequence of five strong motions scaled to reach large displacement demands in the BRBs and, at the same time, to represent different types of motions (near field motions, far-field motions, motions with pulses, and motions in soft soils); and in case the bridge does not fail, 4) a sequence of two extreme motions that represents the case of a bridge with rigid piers that is represented with shake tables moving synchronized. The design of the specimen and the testing protocol made it possible: to provide a more stringent testing protocol than qualification hysteretic test protocol, even expanding it to 3-D; to test various types of connections and BRBs for all the applied earthquake histories; to validate the design for the combination of thermal and seismic life demands, and; to quantify the ultimate hysteretic energy capacity of BRBs in terms of cumulative inelastic deformation. Figure 3-17 shows the specimen set up on top of both shake tables.

Figure 3-17: Specimen set up on top of the two shake tables

3.2.1 BRB Configuration

In the bridge specimen, BRBs were installed in two different configurations. Both have BRBs in the transverse and longitudinal direction. In the longitudinal direction of Configuration I, the two BRBs are almost horizontal, as shown in Figure 3-18. In the longitudinal direction of Configuration II, the two BRBs are at an angle of 30 degrees from the horizontal, as shown in Figure 3-19. In both configurations; in the longitudinal direction, the connection of one BRB was bolted and the other was pinned, and; in the transverse direction, all BRBs had bolted connections. Some results from the data analysis are presented in the next sections.

a) 

b) 

Figure 3-18: Specimen with BRBs and instrumentation for Configuration I: a) transverse BRB in the west end, b) longitudinal BRB

a)  b) 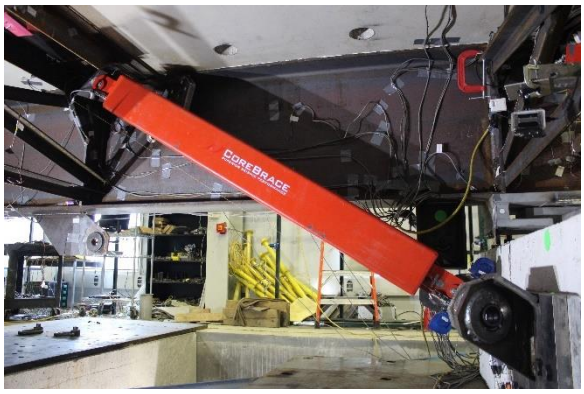

Figure 3-19: Specimen with BRBs and instrumentation for Configuration II: a) transverse BRB in the west end, b) longitudinal BRB

3.2.2 Configuration I

In this section, some test results for Configuration I are presented. Figure 3-21 shows hysteretic loops for all BRBs for ground motions representing the design spectrum and Figure 3-20 shows a preliminary hysteretic loop of one failed BRB. The force in the BRBs were approximated from strain gauges strategically installed on the BRBs. When comparing the force obtained from strain gauges with the inertia force obtained from accelerometers, both are in good agreement, as shown in Figure 3-22. In this configuration one BRB failed after testing the set of ground motions representing the design level, the history representing temperature cycles, and a few strong ground motions. The two other BRBs failed after testing all motions. The maximum BRB demands obtained are summarized in Table 3.

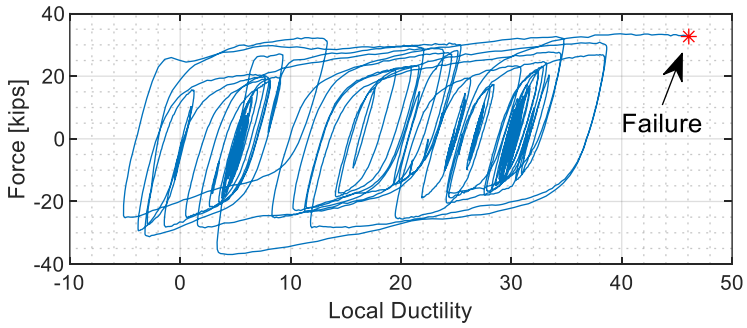

Figure 3-20: Preliminary hysteretic loop of a BRB from a few ground motions before its failure (note: this is "truncated" data; for clarity, the hysteretic curves corresponding to all the ground motions tests applied to this BRB are not all included in this figure)

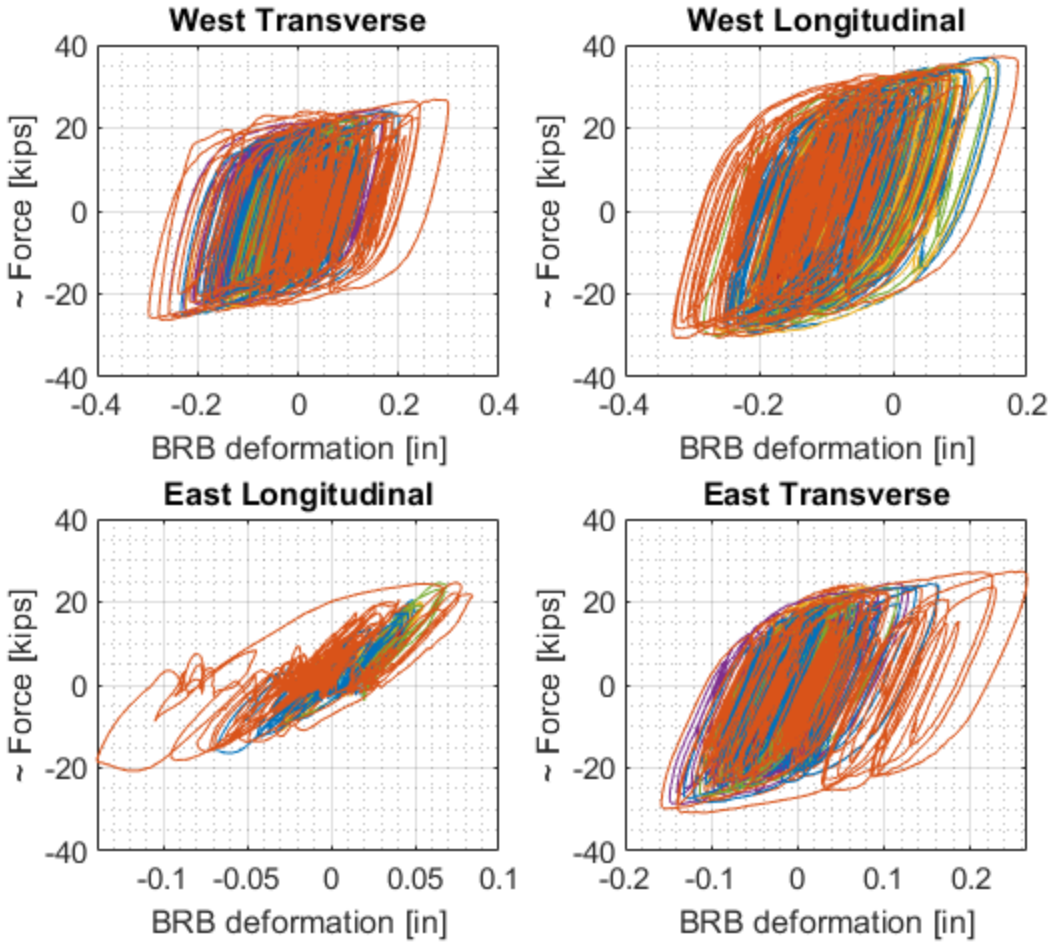

Figure 3-21 BRB hysteretic loops for the steps 1 – 61 for Configuration I

Demands from motions at the design level are shown in Table 1 and are compared with demands expected from numerical analysis. In general demands from numerical analysis are smaller than those obtained from experiment. This is consistent with the fact that it was also observed (not shown here) that the backbone curve of the BRB model used in numerical analysis was contained inside the envelope of the experimentally obtained hysteretic curves. Figure 4 shows cumulative BRB residual displacements, where each test of the specimen is referred to as a "test step". By test step 70, all design level ground motions had been applied, and residual displacements are shown to be negligible. Residual displacements were generally small after each individual earthquake, and the cumulative residual displacements before failure remained less than 20 times the BRB yield deformation for cases where BRBs reached core ductilities of up to 30. Figure 3-24 shows that, for each of the ground motions tested, cumulative plastic deformation demands were generally less than 200 times the BRB yield deformation, except for one earthquake (namely, the Puebla 2017, Mexico, earthquake). Results also showed that deformations due to temperature cycles induced smaller

fatigue demands in BRBs than earthquakes. Finally, none of the various BRB connections used showed instability during testing and maximum demands while the BRBs yielded in compression are presented in Table 3.

Table 1: Mean deformation in BRBs from NL-RHA (inches) compared to experimental values for spectral matched ground motions

BRB	WT	WL	EL	ET
Numerical Model	0.17	0.29	0.07	0.22
Experiment	0.19	0.22	0.06	0.14

* WL: west longitudinal BRB, EL: east longitudinal BRB, WT: west transverse BRB, ET: east transverse BRB

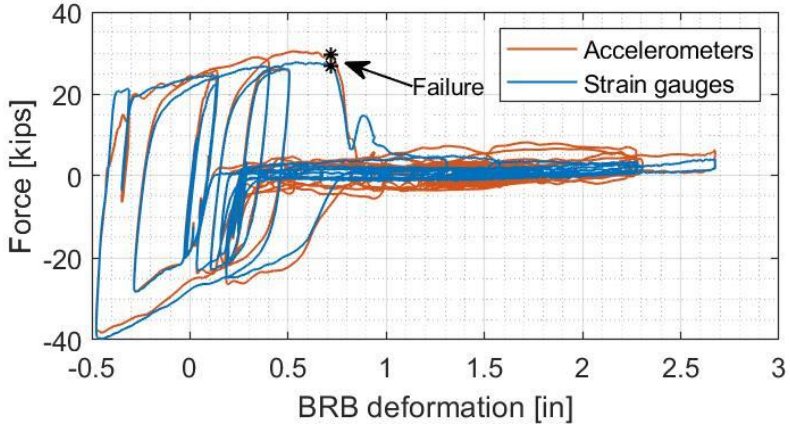

Figure 3-22 West transverse BRB hysteretic loops for the failure step (Step 95) with forces approximated from strain gauges and inertia force

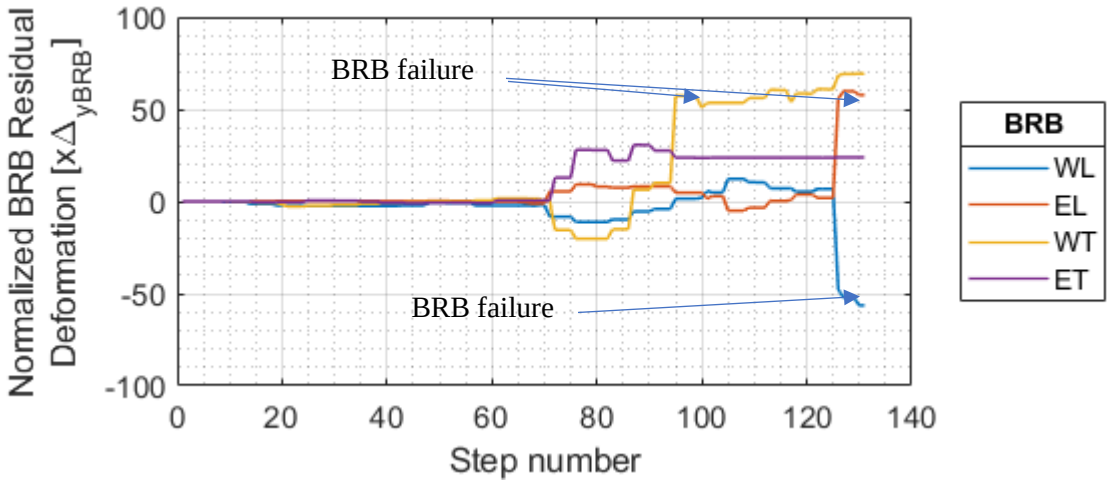

Figure 3-23: Normalized residual BRB deformations (WL: west longitudinal BRB, EL: east longitudinal BRB, WT: west transverse BRB, ET: east transverse BRB)

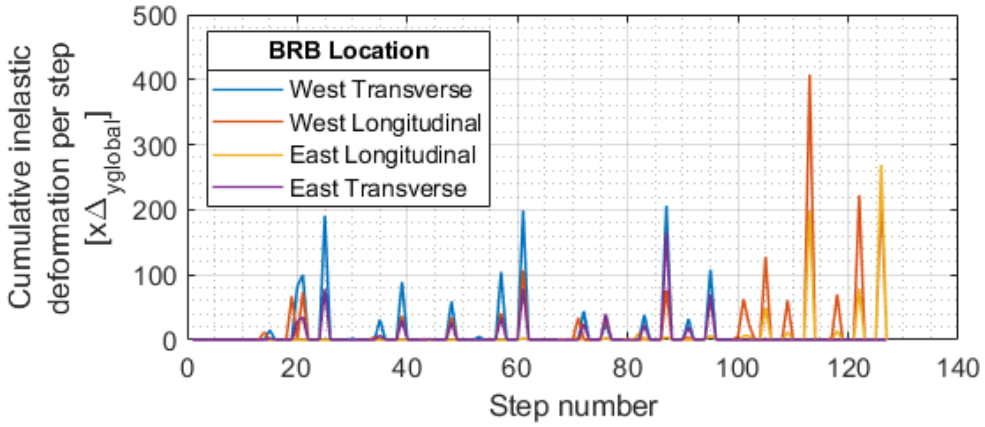

Figure 3-24 BRB cumulative inelastic deformation per step for Configuration I

Table 2: Maximum connections demands in Configuration I while BRBs were yielding in compression

Description	BRB location			
	WT	WL	EL	ET
Horizontal out-of-plane displacement [in]	0.95	2.1	1.3	0.08
Distance between hinges for vertical rotation [in]	56	74	69	57
H. Angle [x10^{-2} rad]	0.017	0.028	0.019	0.014
H. Angle [deg]	0.97	1.60	1.08	0.80
Vertical component displacement [in]	--	--	--	0.57
Distance between hinges for horizontal rotation [in]	--	--	--	42
V. Angle [x10^{-2} rad]	--	--	--	0.126
V. Angle [deg]	--	--	--	0.7

Note: WN = West north BRB, WS = West south BRB, EN = East north BRB, ES = East south BRB

3.2.3 Configuration II

This configuration performed similarly to Configuration I. In comparison with Configuration I, this configuration was tested twice for ground motions representing the design level. The first time only horizontal components of ground excitation were considered, and the second time vertical components were also included. Comparison of numerical and experimental demands are shown in Table 4. After one BRB failed, it was replaced in step 68 by the BRB 1a that did not fail in Configuration I before resuming the test. Cumulative inelastic deformations are shown in Figure 3-25. Note that generally no single history used generated more than 200 times the global yield deformation (the largest was 190), with exception of the Puebla, 2017, Mexican RP motion at 100% scale, and except for the results for the replaced BRB (west

transverse from Step 68 to 77). Maximum demands in connections while the BRB was yielding in compression are presented in Table 5. Finally, the maximum demands in BRBs (without considering the replaced BRB) are presented in Table 6.

Table 3: Summary of maximum BRB demands for Configuration I

Description	WT	WL	EL	ET
BRB number	2a	3a	4a	1a
Max. deformation [in]	0.72	1.94	1.55	1.22
Min. deformation [in]	-0.77	-0.84	-1.59	-0.16
Max def. amplitude [in]	1.49	2.78	3.14	1.38
Max core strain	3.4%	5.5%	4.4%	6.3%
Min core strain	-3.6%	-2.4%	-4.5%	-0.8%
Amplitude core strain	7.0%	7.9%	8.9%	7.1%
Amplitude normalized by core yielding strain	53	60	68	54
Cumulative inelastic deformation	1332	1793	671	664
Max. force (Tension) [kip]	31	46	36	33
Max. force (Compression) [kip]	40	46	40	35
ω	1.63	2.01	1.89	1.73
$\omega\beta$	2.10	2.01	2.01	1.84
Status	Failed	Failed	Failed	----

Note: WT = West transverse BRB, WL = West Longitudinal BRB, ET = East longitudinal BRB, ET = East transverse BRB

Table 4 Mean apparent BRB deformation in inches

Description	BRB location			
	WT	WL	EL	ET
Analytical result for motions at 100%, no vertical	0.19	0.27	0.07	0.24
Experiment E08-E07 100% - with vertical	0.18	0.27	0.10	0.16
Experiment E01-E04 100% - no vertical	0.20	0.26	0.09	0.17
Ratio experimental to analytical, no vertical	1.05	0.96	1.29	0.71
Ratio experimental with vertical to without vertical	0.90	1.04	0.9	0.94

b)

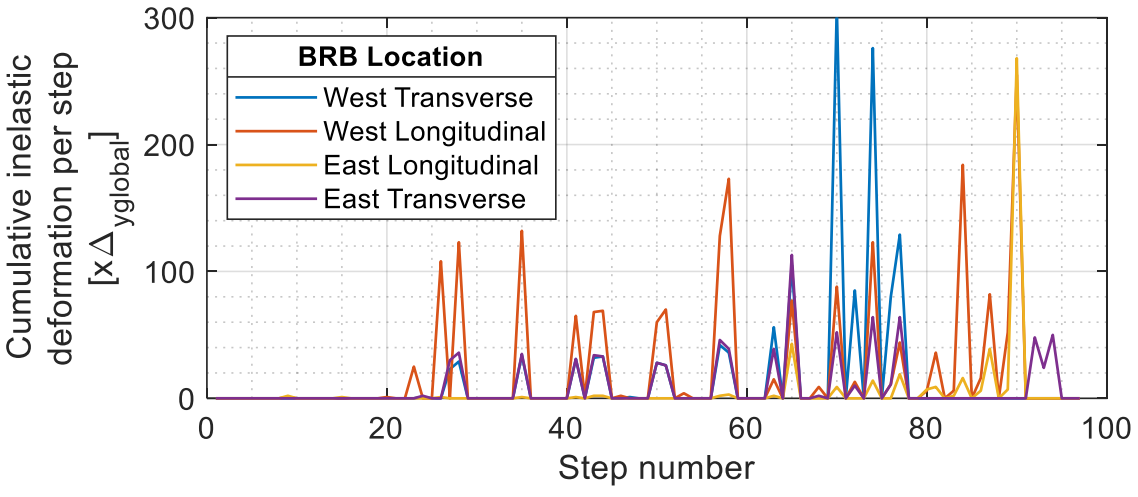

Figure 3-25 Cumulative inelastic deformation in each step for Configuration II

Table 5 Maximum connection demands for Configuration II while BRBs were yielding in compression

Description	BRB location			
	WT	WL	EL	ET
Maximum step considered	65	90	90	97
Horizontal out-of-plane displacement [in]	0.70	3.48	2.13	1.05
Distance between hinges for vertical rotation [in]	56.00	73.75	76.00	55.75
H. Angle [x10^{-2} rad]	1.25	5.20	2.80	1.88
H. Angle [deg]	0.72	2.98	1.60	1.08
Bending strain due to horizontal displacement [μin/in]	900	1400	1200	730
Vertical component displacement [in]	0.25	0.76	--	0.45
Distance between hinges for horizontal rotation [in]	42.00	53.75	--	55.75
V. Angle [x10^{-2} rad]	0.60	1.40	--	0.81
V. Angle [deg]	0.30	0.81	--	0.46
Strain due to vertical displacement [in/in]	1000	1800	--	--

* WN = West north BRB, WS = West south BRB, EN = East north BRB, ES = East south BRB

Table 6 Summary of extreme BRB demands for Configuration II original BRBs

Description	WT	WL	EL	ET
BRB number	1b	5a	6a	2b
Max. deformation [in]	0.50	1.10	0.35	0.93
Min. deformation [in]	-0.43	-0.85	-1.52	-0.19
Max def. amplitude [in]	0.93	1.95	1.87	1.13
Max core strain [%]	2.58	3.82	1.16	4.40
Min core strain [%]	-2.21	-2.95	-4.97	-0.90
Amplitude core strain [%]	4.79	6.77	6.13	5.30
Expected core yielding strain [%]	0.18	0.13	0.13	0.18
Normalized amplitude by core yielding strain	26.2	51.6	46.7	29.1
Cumulative inelastic deformation	477	2047	456	817
~ Max. force (Tension) [kip]	37.7	43.5	35.1	46.1
~ Max. force (Compression) [kip]	47.6	59.1	58.2	40.7
ω	1.42	1.63	1.59	1.74
$\omega\beta$	1.80	2.21	2.63	1.54
Final status	Failed	Failed	Failed	---

* WN = West north BRB, WS = West south BRB, EN = East north BRB, ES = East south BRB

3.2.4 Summary of Experimental Results

Overall, the results obtained for Configurations I and II indicate that the design procedure proposed is acceptable given its simplicity, and is conservative as it led to a design that resulted in predicted demands slightly larger than those observed during testing. Furthermore, by increasing the severity of the ground excitations to push the specimen to failure, it was demonstrated that the BRBs could develop core ductilities greater than 20.

Moreover, it was observed that the temperature effects are small in comparison with demands imposed by seismic motions for this particular configuration/design. The fact that temperature effects did not control the design performance was achieved by an adequate selection of the length of the BRB. Based on the numerical analysis and experimental results, if the deformation amplitude demanded by temperature cycles is in the range of two times the BRB global yield displacement, the temperature cycles over the 75-year service life of the bridge will not have any negative impact on the seismic performance of the bridge.

Regarding the various types of connections used, they all provided adequate support for the BRBs in terms of strength (transferring forces) and stability (providing development of rotation capabilities under full loading.

3.3 DESIGN GUIDELINE – EQUIVALENT LATERAL FORCE METHOD

The following design procedure is proposed for review and possible implementation by AASHTO and Departments of Transportation in their respective seismic design specifications. Note that design requirements are already present in some design specifications for ductile end diaphragms to resist seismic excitations transversally to the axis of bridges. The language provided below is for seismic excitation longitudinally to the axis of bridges, thus complementing the existing information and making possible a complete bi-directional ductile end diaphragm concept.

Design of BRBs in the longitudinal direction

1. Ductile diaphragms designed with Buckling Restrained Braces connecting spans to abutments and piers, for simply supported spans supported by slider bearings, shall be designed using forces, F_i, determined by the following Equivalent Lateral Force Method as follows

$$F_i = \frac{W\ Sa(T)}{R}\ \frac{m_i\phi(x_i)}{\sum_{j=1}^{N_{span}} m_j\phi(x_j)}$$

where i is equal to an integer representing location the ith span and is taken as $(i + 0.5)$ when representing location of the pier cap mass in between the i^{th} and $(i+1)^{th}$ span, m_i is the mass of the i^{th} element, W is the total weight of the bridge, R is the response modification factor, $Sa(T)$ is the spectral acceleration in units of gravity, N_{span} is the number of spans, and x is a normalized distance that represent the position of the center of mass of each span along the length of the bridge, set at zero at mid-length of the bridge and to +1 and -1 at opposite bridge ends, and is defined as:

$$x = 1 - 2\frac{i-1}{N_{span}-1}$$

2. Additional parameters are defined as

$$\gamma = \frac{T_p}{T_{SDOF}}$$

$$\lambda = 1 - \frac{8}{\gamma^2 + 8}$$

$$\eta = \frac{T}{T_{SDOF}} = 1 + 0.4 \cdot \lambda \cdot N_{span}$$

where

$$T_p = 2\pi\sqrt{\frac{M_{span}}{K_{pier}}}$$

and T_{SDOF} is the period of a 1-span bridge with mass equal to the median span mass of the multi-span bridge and designed to reach the target ductility and target maximum deformation in BRBs.

3. The approximate fundamental period of the structure (T), in seconds, shall be determined from the following equation

$$T = \eta \cdot T_{SDOF}$$

4. The equivalent mode shape, ϕ, shall be determined from the following equation

$$\phi(x) = 1 + y(x, k_1) - y(x, k_2)$$

where

$$y(x,k) = 1 - \left(0.6 + \frac{\mu}{100}\right)\left[1 - \left(1 - \frac{|x|^{\frac{1}{k}}}{1.1}\right)^k\right]$$

$$k_1 = 4 \cdot \lambda \leq 0.15(10 + \mu)(1 - 0.7^{N_{span}-2})$$

$$k_2 = 0.06 \cdot (\gamma - 1) > 0$$

and μ is the target ductility expected in BRBs. μ shall be taken between 5 and 10.

5. The R value shall be calculated using the following equations

$$R(T) = \begin{cases} \left(\frac{\mu}{\alpha_u \gamma_\mu} - 1\right)\frac{T}{1.25T_s} + 1 & if\ T < 1.25T_s \\ \frac{\mu}{\alpha_u \gamma_\mu} & otherwhise \end{cases}$$

where

$$\alpha_u = 0.06\mu_{SDOF} + 0.7 \geq 1 \quad \text{if } \mu \leq 10$$

$$\gamma_\mu = \frac{\mu_{max}}{\mu_{SDOF}} = 2\eta - 1 \leq 2.0$$

Note that T_{SDOF} shall be calculated assuming $\eta = 1$.

6. Both group of BRBs connected on each side of the pier caps shall have the same group strength

7. The Buckling Restrained Brace cross-section area shall not be smaller than half the cross-section area calculated for the same bridge considering infinitely rigid piers.

3.3.1 Design example for BRBs

To demonstrate the procedure described above, it was assumed that a regular straight 5-span bridge has to be designed with BRBs in the longitudinal direction for a seismic region where the seismic design spectrum is the one shown in Figure 2-1. Initially, the bridge was analyzed as a multi-span bridge without considering seismic forces. The weight of each floating span was calculated to be 386 kips (equal to a mass of 1 $kip \cdot s^2/in$). The stiffness of piers was assumed to be 100 kip/in. The base of all piers is fixed, and the top is simply connected to spans using slider bearings and BRBs. The lumped mass at the top of the pier is assumed equal to 38.6 kips (10% of the span mass). The target ductility demand in the BRB is selected to be 10, the length of each BRB yielding core is 80in, and their yield strength is $50\ ksi$. The calculated parameters in each iteration are provided in a table below. Design proceed as follows.

1. Definition of the global target ductility expected in BRBs, BRB yield deformation, target BRB deformation, and mean span mass and mean pier stiffness:

$$\Delta_{max} = 1.38\ in$$

$$\Delta_y = 0.138\ in$$

$$\mu = \frac{\Delta_{max}}{\Delta_y} = 10$$

Since the bridge is regular, the mean span mass, M_{span}, is equal to 1 $kip \cdot s^2/in$; and the mean pier stiffness, K_{pier}, is equal to 100 kip/in.

2. Design of a SDOF system with mass equal to the span mass and a target displacement equal to Δ_{max}.

2.1. Calculation of the period of a SDOF system that reach the target deformation.

2.1.1. Value of γ_μ with η equal to 1 (valid for a SDOF).

$$\gamma_\mu = \frac{\mu_{max}}{\mu_{SDOF}} = 2\eta - 1 \leq 2.0$$

$$\gamma_\mu = 2 \cdot (1) - 1 = 1$$

$$\gamma_u = 1 \leq 2 \quad O.K.$$

2.1.2. Value of α_μ

$$\alpha_u = 0.06\mu_{SDOF} + 0.7 \geq 1 \quad \text{if } \mu \leq 10$$

$$\alpha_u = 0.06 \cdot (10) + 0.7 = 1.3 \geq 1$$

$$\alpha_u = 1.3 \geq 1 \quad O.K.$$

2.1.3. Value of T_s

$$T_s = \frac{0.3371}{0.8833} = 0.3816\ s$$

2.1.4. Definition of the values of the equation used to calculate R

$$R(T) = \begin{cases} \left(\frac{\mu}{\alpha_u \gamma_\mu} - 1\right)\frac{T}{1.25T_s} + 1 & if\ \ T < 1.25T_s \\ \frac{\mu}{\alpha_u \gamma_\mu} & otherwhise \end{cases}$$

$$R(T) = \begin{cases} \left(\frac{10}{1.3} - 1\right)\frac{T}{1.25 \cdot (0.3816)} + 1 & if\ \ T < 1.25T_s \\ \frac{10}{1.3} & otherwhise \end{cases}$$

$$R(T) = \begin{cases} 14.03 \cdot T + 1 & if\ \ T < 0.477\ s \\ 7.69 & otherwhise \end{cases}$$

2.1.5. Calculation of the SDOF period by a graphical method. Figure 3-26 shows the spectral acceleration for the design elastic spectrum and for the spectrum divided by R, and the corresponding displacement spectrum obtained from the acceleration spectrum. For a deformation equal to Δ_{max} and to reach a target ductility equal to 10, the period of the SDOF system should be T_{SDOF} and is obtained from the figures using the reduced displacement spectrum (i.e., S_d/R). The period of the SDOF is then used to find the reduced spectral acceleration. These results are provided below:

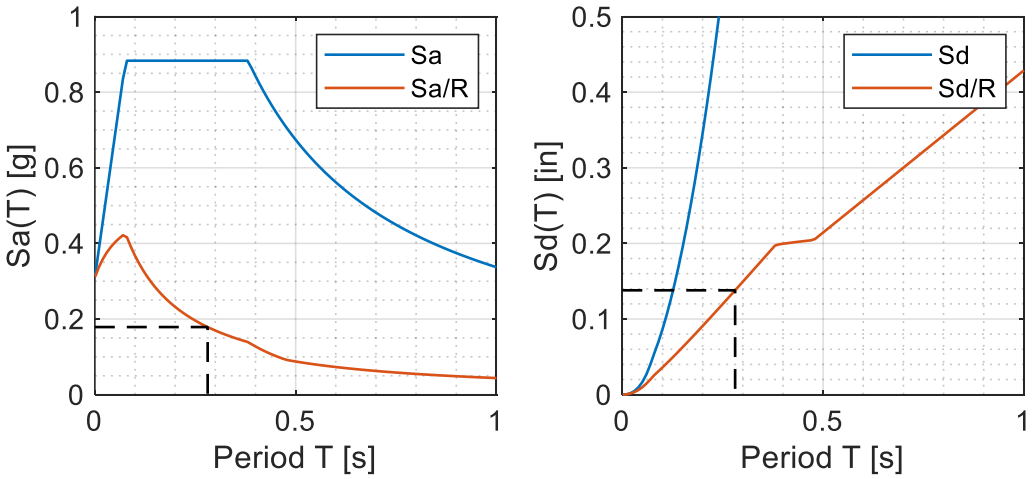

Figure 3-26 Graphical solution: [left] spectral acceleration, [right] spectral displacement

$$T_{SDOF} = 0.281\ s$$

$$Sa_{SDOF}/R = 0.179\ g$$

2.2. Definition of the minimum BRB cross-section area along the bridge. For this step, BRBs have to be designed for one span represented by the SDOF. Two BRBs are considered, one at each end. For a SDOF, the force in each BRB located at the end of the span is

$$F_{BRB_{SDOF}} = \frac{1}{2}\frac{Sa_{SDOF}}{R}\, W_{span} = \frac{1}{2}\cdot 0.179 \cdot 386\ kips = 34.54\ kips$$

The cross-section area of each BRB is

$$A_{BRB_{SDOF}} = \frac{F_{BRB_{SDOF}}}{F_y} = \frac{34.54\ kips}{50\ ksi} = 0.7\ in^2$$

The minimum BRB cross-section area along the bridge is

$$A_{BRB_{min}} = \frac{A_{BRB_{SDOF}}}{2} = \frac{0.7in^2}{2} = 0.35\ in^2$$

3. Calculation of the parameter T_p, γ, λ, and η

$$T_p = 2\pi\sqrt{\frac{M_{span}}{K_{pier}}} = 2\pi\sqrt{\frac{1\ kip\cdot s^2/in}{100\ kip/in}} = 0.63\ s$$

$$\gamma = \frac{T_p}{T_{SDOF}} = \frac{0.63\ s}{0.281\ s} = 2.242$$

$$\lambda = 1 - \frac{8}{\gamma^2 + 8} = 1 - \frac{8}{2.242^2 + 8} = 0.386$$

$$\eta = 1 + 0.4\cdot\lambda\cdot N_{span} = 1 + 0.4\cdot(0.386)\cdot(5) = 1.772$$

4. Approximation of the fundamental period of the bridge, T

$$T = \eta\cdot T_{SDOF} = 1.772\cdot 0.281\ s = 0.498\ s$$

5. Calculation of the reduction factor for the multi-span bridge.

5.1.1. Value of γ_μ.

$$\gamma_\mu = \frac{\mu_{max}}{\mu_{SDOF}} = 2\eta - 1 \le 2.0$$

$$\gamma_\mu = \min[2\cdot(1.772) - 1\ , 2] = \min[2.54\ , 2] = 2$$

5.1.2. Reduction factor. Since $T \ge 1.25T_s$ then

$$R = \frac{\mu}{\alpha_u\cdot\gamma_\mu} = \frac{10}{(1.3)\cdot(2)} = 3.85$$

6. Calculation of the reduced spectral acceleration

$$\frac{Sa(T)}{R} = \frac{0.678}{3.85} = 0.176\ g$$

7. Definition of the equivalent mode shape

7.1. Value of k_1

$$k_1 = 4 \cdot \lambda = 4 \cdot (0.386) = 1.544 \leq 0.15(10 + \mu)(1 - 0.7^{N_{span}-2})$$

$$k_1 = 1.544 \leq 0.15(10 + \mu)(1 - 0.7^{N_{span}-2})$$

$$k_1 = 1.544 \leq 0.15 \cdot (10 + 10) \cdot (1 - 0.7^{5-2}) = 1.971$$

$$k_1 = 1.544 \leq 1.971$$

$$k_1 = 1.544$$

7.2. Value of k_2

$$k_2 = 0.06 \cdot (\gamma - 1) > 0 = \max\left[0.06 \cdot (\gamma - 1)\ , 0\right]$$

$$k_2 = \max[0.06 \cdot (2.242 - 1)\ , 0] = \max\left[0.0745\ , 0\ \right]$$

$$k_2 = 0.0745$$

7.3. Definition of the equation of the mode shape

$$y(x,k) = 1 - \left(0.6 + \frac{\mu}{100}\right)\left[1 - \left(1 - \frac{|x|^{\frac{1}{k}}}{1.1}\right)^{k}\right] = 1 - \left(0.6 + \frac{10}{100}\right)\left[1 - \left(1 - \frac{|x|^{\frac{1}{k}}}{1.1}\right)^{k}\right]$$

$$y(x,k) = 1 - 0.7\left[1 - \left(1 - \frac{|x|^{\frac{1}{k}}}{1.1}\right)^{k}\right] = 0.3 + 0.7\left(1 - 0.909 \cdot |x|^{\frac{1}{k}}\right)^{k}$$

$$\phi(x) = 1 + y(x,k_1) - y(x,k_2)$$

$$\phi(x) = 1 + 0.7\left(1 - 0.909 \cdot |x|^{\frac{1}{k_1}}\right)^{k_1} - 0.7\left(1 - 0.909 \cdot |x|^{\frac{1}{k_2}}\right)^{k_2}$$

8. Calculation of the equivalent lateral forces. The equivalent forces are presented in Table 3-7. Figure 3-27 is a sketch that shows graphically the shape of the mode shape and the distribution of forces.

Table 3-7 Calculation of equivalent lateral forces

Element	Mass (m) $[kip \cdot s^2/in]$	x	$\phi(x)$	$m \cdot \phi(x)$	$\frac{m_i\phi(x_i)}{\Sigma m_j\phi(x_j)}$	$F_i = \frac{W\,Sa(T)}{R}\frac{m_i\phi(x_i)}{\Sigma m_j\phi(x_j)}$ [kip]
Span 1	1.0	-1.00	0.432	0.432	0.1421	52.13
Top pier 1	0.1	-0.75	0.382	0.038	0.0126	4.62
Span 2	1.0	-0.50	0.484	0.484	0.1595	58.51
Top pier 2	0.1	-0.25	0.644	0.064	0.0212	7.78
Span 3	1.0	0.00	1.000	1.000	0.3293	120.81
Top pier 3	0.1	0.25	0.644	0.064	0.0212	7.78
Span 4	1.0	0.50	0.484	0.484	0.1595	58.51
Top pier 4	0.1	0.75	0.382	0.038	0.0126	4.62
Span 5	1.0	1.00	0.432	0.432	0.1421	52.13
	5.4			3.037	1.0000	366.89

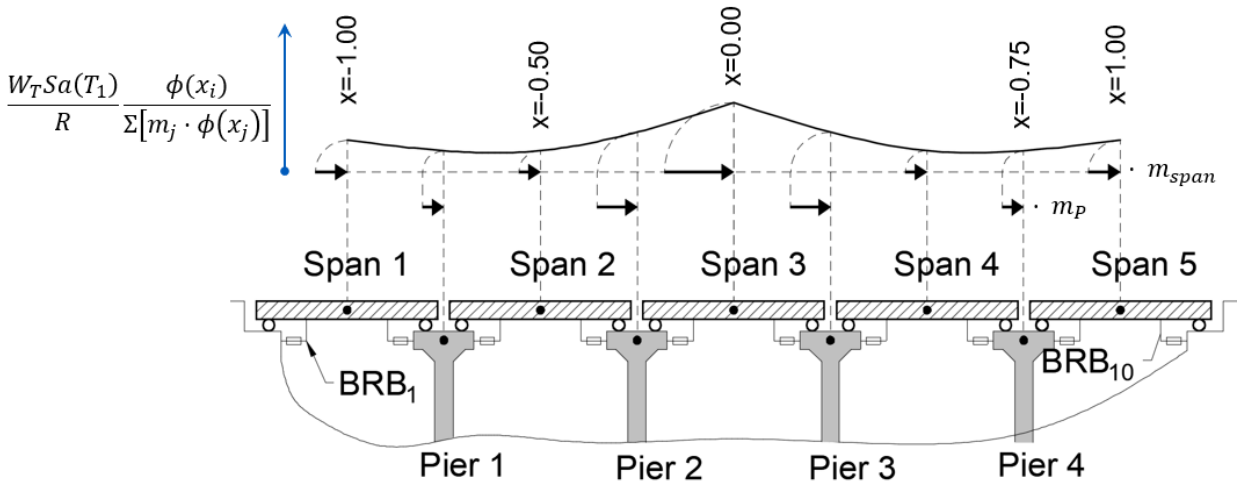

Figure 3-27 Graphical representation of the equivalent mode shape and equivalent forces

9. With the forces calculated in the previous step, the BRB cross-section areas are obtained by an iterative procedure. Any structural software could be used to calculate the forces in BRBs. For the first iteration (labeled "iteration 0"), $A_{BRB_{SDOF}}$ is used as the cross-section area for all BRBs, but any cross-section area could be used in iteration 0. Forces in BRBs are calculated and the cross-section area is updated, then the model is updated with the new areas to recalculate forces in BRBs and redesigning them, and

the process is repeated until convergence is reached. For this example, four iterations were required to reach convergence. Cross-section area for each iteration are shown in Table 3-8. If the mass of the pier cap would be included in the step 3, the resulting cross-section areas would be between 1% to 5% smaller than those obtained in Table 3-8.

Table 3-8 BRB cross-section areas [in²]

BRBs connected to	Iterations				
	0	1	2	3	Final Design
Abutments	0.7	1.552	2.064	2.246	2.317
Pier 1	0.7	1.225	1.522	1.625	1.666
Pier 2	0.7	1.211	1.211	1.211	1.211

10. Check of minimum BRB cross-section areas. As observed in Table 3-8, all areas are larger than $A_{BRB\,min}$; therefore, cross-section areas in the table are used.

4 PLANS FOR IMPLEMENTATION

This NCHRP IDEA Type 2 project was conducted to validate the proposed bi-directional ductile diaphragm to a point ready to transition this technology to field applications. The scale-model testing of the bridge span using two shake tables fulfilled this objective by verifying the dynamic response of a complete system in which the bi-directional ductile diaphragm concept was implemented. BRBs with various configurations and various connections details were sequentially validated as part of this shake-table test series. The simple design procedure proposed and validated as part of this research project can be used in design guidelines for the bidirectional ductile diaphragms to resist earthquakes from any directions. The simple equations proposed are adequate for implementation by AASHTO (via T3 Seismic and T14 Steel Design) and by Departments of Transportation. Accordingly, this report will be shared with the chairs of the T3 and T14 committees that shepherd these design specifications. In particular, the information will be shared with the California Department of Transportation (Caltrans) for review and possible inclusion into its "Seismic Design Specifications for Steel Bridges" (at the time of this writing, the 2nd Edition (2015) of this document is being reviewed for an upcoming 3rd Edition). Furthermore, the findings from this research project will be published in a set of peer-reviewed papers in the leading publications in the field, and will be presented at top level conferences. In particular, it is planned to provide such a presentation at the 2024 TRB meeting in D.C. Finally, the project PI is frequently asked to give presentations on the topic of resilience and on how to achieve/design resilient structures, and the findings of this research project will be integrated into these presentations to various groups and agencies.

5 CONCLUSIONS

Analytical results from this project have provided the missing design procedure for the longitudinal direction required to design bidirectional ductile end diaphragms. This simple design procedure developed to facilitate the design of these resilient bridges has been validated using non-linear inelastic time history analyses, and has been cast in a format ready for adoption by bridge design specifications. Additionally, the experimental part of the project, evaluated the concept and different connections details through shake table testing. Results from experiments showed that the concept can to provide seismic resilient bridges and that thermal expansion is not controlling the design of this system. As a byproduct, all details considered to transfer forces from BRBs to the substructure and to the superstructure performed well, making them adequate to be used with BRBs in Bidirectional Ductile End-Diaphragms.

As such, and taken together, the analytical, numerical, and experimental studies conducted here have demonstrated that bridges using the bidirectional ductile end diaphragm concept with BRBs can have piers protected from damage, limited displacement demands to prevent unseating or pounding of spans (and allowing the use of common/standard expansion joints), and no damage to the BRBs. Therefore, these bridges would experience no loss of functionality following an earthquake. As such, the end result is a fully resilient bridge that remains in service throughout and after the earthquake.

In short, this research made the Bidirectional Ductile End-Diaphragms concept using BRBs ready for adoption by bridge design specifications.

Future research could be conducted to: (i) provide a design procedure similar to the one used here but formulated specifically for the case when BRBs are installed in a “V” configuration, and; (ii) to expand the ductile diaphragm concept to skew and/or curved simply supported multi-span bridges.

6 INVESTIGATORS' PROFILES

6.1 MICHEL BRUNEAU

SUNY Distinguished Professor Michel Bruneau is recognized nationally and internationally for the impact of his research contributions to the design and behavior of steel structures subjected to earthquakes and blasts (and development/testing of hysteretic energy dissipating devices of the type considered in this proposal). He has a proven track record of research accomplishments producing practical outcomes and design equations for innovative structural systems. For example, his development and validation of the tubular eccentrically braced frames concept for bridges was implemented in the $1B temporary supports of the new San-Francisco Oakland Bay Bridge. Likewise, much of his work has also been included in design standards or specifications (such as the AASHTO Guide Specifications for LFRD Seismic Bridge Design and the Canadian Highway Bridge Design Code, to name a few), leading to implementation in countless structures worldwide. He has authored over 600 technical publications, including over 180 articles in the leading peer-reviewed journals in his field. He is one of the most cited researchers in structural engineering and earthquake engineering. Notably, he is the lead author of the 900-pages textbook "Ductile Design of Steel Structures," used worldwide by structural engineers and considered by many to be the reference for the seismic design of steel structures.

The PI has received several awards and recognitions for his work and has been inducted as a fellow of the Canadian Academy of Engineering. He is also a Distinguished Member of ASCE and a member of various AISC and CSA committees developing design specifications for bridges and buildings, including the Seismic Committee of the Canadian Highway Bridge Design Code. He also served on the NCHRP Project 12-49 that developed "Guide Specifications for the Seismic Design of Bridges," in parts integrated into the 2009 AASHTO Guide Specifications for LFRD Seismic Bridge Design. He has conducted numerous reconnaissance visits to disaster-stricken areas and has served as Director of MCEER, a national research center that focused on the development of disaster resilient structures. A detailed outline of qualifications is available at www.eng.buffalo.edu/~bruneau.

6.2 HOMERO CARRION CABRERA

Homero Carrion obtained his Bachelor degree in Civil Engineering (with honors) at the Universidad de Cuenca, Ecuador, and his Master degree in Engineering (with honors) with major in Structural Engineering at the Universidad Nacional Autonoma de Mexico (UNAM). He obtained his Master of Science degree and Ph.D. in Structural and Earthquake Engineering from the Department of Civil, Structural, and Environmental Engineering at the University at Buffalo.

His M.Eng. studies were funded by Mexican (CONACYT) and Ecuadorian (SENESCYT) scholarships. He received a Fulbright-SENESCYT fellowship for his studies at the University at Buffalo (UB). During his Ph.D. studies, he also received the Dean's Graduate Achievement Award from the School of Engineering and Applied Sciences.

His research interests include the study of mechanical behavior of materials, dynamics of structures and seismic performance-based design. His bachelor's thesis was focused on viscoelastic materials and optimization methods; and in his master's thesis, he studied the behavior of concrete columns in seismic regions focusing on their shear strength. After his master, he became an assistant professor (lecturer) at the Universidad de Cuenca and the Universidad Catolica de Cuenca (in his city) where he taught a number of courses, including "Dynamics and seismic design of structures". During his studies at UB, he focused on the seismic behavior of structures, using nonlinear time history analysis to evaluate the performance and design complex structures.

7 REFERENCES

1) Enke, David L, Chakkaphan Tirasirichai, and Ronaldo Luna. 2008. "Estimation of earthquake loss due to bridge damage in the St. Louis metropolitan area. II: Indirect losses." *Natural Hazards Review* 9 (1):12-19.
2) Aiken, ID, Peter Clark, Frederick Tajirian, Kazuhiko Kasai, Isao Kimura, and Eric Ko. 1999. "Unbonded braces in the United States—Design studies, large-scale testing, and the first building application." Proceedings of the International Post-SMiRT Conference Seminar, Korea Earthquake Engineering Research Center, Volume I, pp. 317-337.
3) AISC 341. 2022. *Seismic Provisions for Structural Steel Buildings, Chicago, Illinois, USA: American Institute of Steel Construction (AISC).*
4) Ingham, TJ, S Rodriguez, and M Nader. 1997. "Nonlinear analysis of the Vincent Thomas Bridge for seismic retrofit." *Computers & structures* 64 (5-6):1221-1238.
5) Lanning, Joel, Gianmario Benzoni, and Chia-Ming Uang. 2016a. "Using buckling-restrained braces on long-span bridges. II: Feasibility and development of a near-fault loading protocol." *Journal of Bridge Engineering* 21 (5):04016002.
6) Lanning, Joel, Gianmario Benzoni, and Chia-Ming Uang. 2016b. "Using buckling-restrained braces on long-span bridges. I: full-scale testing and design implications." *Journal of Bridge Engineering* 21 (5):04016001.
7) CoreBrace. 2021. "Available online at: https://www.corebrace.com/. Accessed January, 2020.".
8) Kanaji, H, N Hamada, T Ishibashi, M Amako, and T Oryu. 2005. "Design and performance tests of buckling restrained braces for seismic retrofit of a long-span bridge." 21th US–Japan bridge engineering workshop. Panel on wind and seismic effects.
9) Zahrai, Seyed Mehdi, and Michel Bruneau. 1999a. "Ductile end-diaphragms for seismic retrofit of slab-on-girder steel bridges." *Journal of structural engineering* 125 (1):71-80.
10) Zahrai, Seyed Mehdi, and Michel Bruneau. 1999b. "Cyclic testing of ductile end diaphragms for slab-on-girder steel bridges." *Journal of structural engineering* 125 (9):987-996.
11) Alfawakhiri, Farid, and Michel Bruneau. 2001. "Local versus global ductility demands in simple bridges." *Journal of Structural Engineering* 127 (5):554-560.
12) AASHTO. 2011. *AASHTO Guide Specifications for LRFD Seismic Bridge Design*. 2nd Edition. Revision 2015. ed: AASHTO.
13) Carden, Lyle P, Ahmad M Itani, and Ian G Buckle. 2006. "Seismic performance of steel girder bridges with ductile cross frames using buckling-restrained braces." *Journal of structural engineering* 132 (3):338-345.
14) Celik, Oguz C, and Michel Bruneau. 2009. "Seismic behavior of bidirectional-resistant ductile end diaphragms with buckling restrained braces in straight steel bridges." *Engineering Structures* 31 (2):380-393.
15) Wei, Xiaone, and Michel Bruneau. 2018. "Experimental investigation of buckling restrained braces for bridge bidirectional ductile end diaphragms." *Journal of Structural Engineering* 144 (6):04018048.
16) Pantelides, Chris P, Luis Ibarra, Yuandong Wang, and Anurag Upadhyay. 2016. Seismic rehabilitation of skewed and curved bridges using a new generation of buckling restrained braces. Mountain Plains Consortium.

17) Wei, Xiaone, and Michel Bruneau. 2016. "Buckling restrained braces applications for superstructure and substructure protection in bridges." State University of New York at Buffalo.
18) FEMA. 2009. Quantification of Building Seismic Performance Factors. edited by California Applied Technology Council for the Federal Emergency Management Agency: Redwood City, USA.
19) McKenna, Frank, Gregory L Fenves, and Michael H Scott. 2000. "Open system for earthquake engineering simulation." *University of California, Berkeley, CA*.
20) Merritt, S., C. M. Uang, and G. Benzoni. 2003. Subassemblage testing of star seismic buckling-restrained braces. La Jolla.
21) Newell, James, Chia-Ming Uang, and Gianmario Benzoni. 2006. Subassemblage Testing of Corebrace Buckling-Restrained Braces (G series). La Jolla.
22) Miranda, Eduardo, and Vitelmo V Bertero. 1994. "Evaluation of strength reduction factors for earthquake-resistant design." *Earthquake spectra* 10:357-357.
23) Riddell, Rafael, Pedro Hidalgo, and E Cruz. 1989. "Response modification factors for earthquake resistant design of short period buildings." *Earthquake spectra* 5 (3):571-590.
24) Priestley, M.J.N., G.M. Calvi, and M.J. Kowalsky. 2007. *Displacement-Based Seismic Design of Structures*. Edited by IUSS PRESS.
25) Harris, Harry G, and Gajanan Sabnis. 1999. *Structural modeling and experimental techniques*: CRC press.
26) AASHTO. 2017. *AASHTO LRFD Bridge Design Specifications*. 8th Edition ed.
27) CoreBrace. 2020. "Available online at: https://www.corebrace.com/project/vancouver-city-hall/. Accessed June, 2020.".
28) Carden, Lyle P, Ahmad M Itani, and Ian G Buckle. 2008. Seismic performance of steel girder bridge superstructures with ductile end cross frames and seismic isolators.
29) Zahrai, Seyed Mehdi, and Michel Bruneau. 1998. "Impact of diaphragms on seismic response of straight slab-on-girder steel bridges." *Journal of Structural Engineering* 124 (8):938-947.
30) AISC 360. 2016. *Specification for Structural Steel Buildings, Chicago AISC*.

8 APPENDIX: RESEARCH RESULTS

SIDEBAR INFO
Program Steering Committee: NCHRP IDEA Program Committee
Month and Year: March, 2023
Title: Achieving Resilient Multi-Span Bridges by using Buckling-Restrained Braces
Project Number: NCHRP-IDEA 215
Start Date: April 1, 2019
Completion Date: March 31, 2023
Product Category: Innovations Deserving Exploratory Analysis (IDEA) Program Highway Final Report
Principal Investigator: Michel Bruneau
Name, Title: SUNY Distinguished Professor
E-Mail: bruneau@buffalo.edu
Phone: (716) 645-3398

TITLE
Seismic Resilient Multi-Span Bridges

SUBHEAD
Minimizing displacement demands and eliminating damage using Buckling Restrained Braces, to achieving immediate post-earthquake functionality

WHAT WAS THE NEED?
Ductile End Diaphragms (DED) is a concept that can prevent damage in the substructure and superstructure of bridges under seismic excitation in the direction transverse (perpendicular) to the bridge longitudinal axis, and that is already implemented in the AASHTO design provisions. These diaphragms are located at the end of the superstructure spans and use hysteretic energy-dissipating devices as "fuses" or sacrificial elements. A Bi-directional Ductile End Diaphragms (BDED) concept was proposed to expand the concept of DED to also prevent damage in bridges due to earthquake excitation in the longitudinal direction. Two main problems that prevented the implementation and broad use of this concept were addressed in this project: (1) the need to understand analytically the behavior of the system in a multi-span configuration, to be able to propose a simple design procedure; and (2) the need to validate experimentally BRB connections to demonstrate their ability to work under 3-D displacements imposed due to the inclination of BRBs.

WHAT WAS OUR GOAL?
The objective was to conduct the analytical and experimental research needed to expand and validate the Bidirectional Ductile Diaphragm concept, developed in an earlier IDEA project (NCHRP-172), for application in common multi-span bridges. Buckling Restrained Braces (BRBs) were used as fuse elements located at the end of a superstructure's floating span for this purpose. This innovative system can provide seismically resilient bridges with damage-free piers at low cost while minimizing displacement demands to levels that can be easily accommodated by conventional expansion joints.

WHAT DID WE DO?
The analytical study initially focused on the behavior in the longitudinal direction of regular bridges having BRBs in BDED to determine the level of complexity required to adequately predict the bridge seismic response, with the goal of providing simple, ready-to-implement, design rules that enable satisfactory seismic performance (to complement the existing AASHTO design provisions for the transverse direction excitation of ductile diaphragms). The nonlinear behavior of bridges designed using various methods was assessed by subjecting them to suites of earthquake motions using non-linear time-history analyses. The impact of the ratio of substructure-to-superstructure stiffness, span length, period, and other factors on

response was quantified such as to keep the substructure and the superstructure elastic and to limit the displacement demands in expansion joints (which also makes it easier to prevent unseating in retrofit situations). One proposed design procedure based on Equivalent Lateral Forces (ELF) was shown to be particularly expedient and effective. It was also determined that, according to fatigue index calculations, it is not necessary to replace BRBs after an earthquake. The proposed design procedures were shown to be adequate for different seismic hazards, BRB geometries, and many irregular bridges.

The experimental study was performed at the University at Buffalo's Structural Engineering and Earthquake Simulation Laboratory. The proposed ELF design procedure and a simple displacement-based design approach was used to design BRBs in BDED in a 5-span prototype bridge in the longitudinal and transverse direction, respectively. The geometry of a prototype bridge was used to design a test specimen that considered various BRB configurations, BRB end-connections to gusset plates, BRB connections to concrete (with details applicable to new structures and/or retrofitted ones), and BRB to steel girder connections. The bridge specimen was supported on two shake tables able to apply both unsynchronized and synchronized excitation representing the demands at the ends of the span. The bridge specimen was tested with different BRB configurations, and was subjected to displacement sequences representing thermal expansion demands, design level seismic demands, and strong motions to represent different types of motions (near field, far field, pulse-type motions, and motions in soft soils). Each BRB configuration was tested until failure.

WHAT WAS THE OUTCOME?

Analytical results from this project provided the missing design procedure for the longitudinal direction required to design bidirectional ductile end diaphragms. Additionally, the experimental part of the project, using a specimen designed per the proposed design procedure, evaluated the concept and different connection details through shake table testing. Results from experiments showed that the concept can to provide seismic resilient bridges and that thermal expansion is not controlling the design of this system. It also demonstrated that pier damage could be prevented and that span displacement demands were small (i.e., of a magnitude that can be accommodated by conventional expansion joints). As a byproduct, all details considered to transfer forces from BRBs to the substructure and to the superstructure performed well, making them adequate to be used BRBs in BDED.

WHAT WAS THE BENEFIT?

This research made the BDED concept ready for adoption by bridge design specifications.

IMAGE

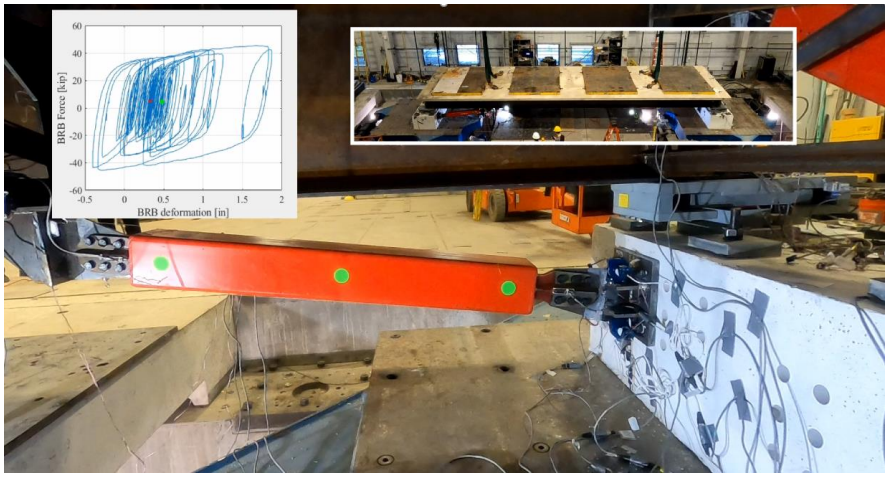

Shake Table test of a resilient bridge span with Buckling Restrained Braces (use QR code to watch video)